4234 J. Med. Chem. 2010, 53, 4234–4247
DOI: 10.1021/jm100233b

Journal of Medicinal Chemistry Article

Mechanism-Based Inhibitors of the Aspartyl Protease Plasmepsin II as Potential Antimalarial Agents

Deepak Gupta,[†,§] Ravikiran S. Yedidi,[‡,∥] Sheeba Varghese,[†,⊥] Ladislau C. Kovari,[‡] and Patrick M. Woster*[,†]

[†]*Department of Pharmaceutical Sciences, Eugene Applebaum College of Pharmacy and Health Sciences, Wayne State University, 3132 Applebaum Hall, 259 Mack Avenue, Detroit, Michigan 48202, and* [‡]*Department of Biochemistry and Molecular Biology, School of Medicine, Wayne State University, Detroit, Michigan 48202.* [§]*Current affiliation: LECOM-School of Pharmacy, Room No. 280, 5000 Lakewood Ranch Boulevard, Bradenton, Florida 34202.* [∥]*Current affiliation: ERS/HAMB-NCI/NIH, 10 Center Drive, Room No. 5A24, Bethesda, Maryland 20892.* [⊥]*Current affiliation: Feik School of Pharmacy, University of the Incarnate Word, 4301 Broadway, Box 99, San Antonio, Texas 78209.*

Received February 22, 2010

Four aspartyl proteases known as plasmepsins are involved in the degradation of hemoglobin by *Plasmodium falciparum*, which causes a large percentage of malaria deaths. The enzyme plasmepsin II (Plm II) is the most extensively studied of these aspartyl proteases and catalyzes the initial step in the breakdown of hemoglobin by the parasite. Several groups have reported the design, synthesis, and evaluation of reversible peptidomimetic inhibitors of Plm II as potential antimalarial agents. We now report four peptidomimetic analogues, compounds **6**−**9**, which are rationally designed to act as mechanism-based inhibitors of Plm II. Three of these analogues produce potent irreversible inactivation of the enzyme with IC_{50} values in the low nanomolar range. Of these three compounds, two retain the low micromolar IC_{50} values of the parent compound in *Plasmodium falciparum* (clone 3D7) infected erythrocytes. These analogues are the first examples of fully characterized mechanism-based inactivators for an aspartyl protease and show promise as novel antimalarial agents.

Introduction

Malaria remains one of the world's most deadly diseases, threatening 40% of the world's population and infecting 300 million people worldwide. In Africa alone, more than one million children under the age of 5 die from malaria each year,[1−3] translating to one death from malaria every 30 s. Human infection can be caused by four distinct species of the protozoon *Plasmodium*, but *P. vivax* and *P. falciparum* account for more than 95% of malaria cases.[4,5] Nearly all deaths caused by malaria are due to infection by *P. falciparum*.[3,4] Malaria has become more difficult to treat because of an increase in multidrug resistant strains.[5] In fact, the re-emergence of malaria as a worldwide epidemic can be largely attributed to the rapid development of parasite resistance. Some progress has been made in identifying resistance markers in parasites that fail conventional therapy.[6−8] The disease is transmitted by the bite of the female anopheles mosquito, at which time sporozoites of *P. falciparum* are discharged into the puncture wound and are carried to the liver, where they enter hepatic mesenchymal cells. Lysis of the hepatocyte then releases the merozoite form of *P. falciparum*, which invades host red blood cells, feeding on hemoglobin during the erythrocytic portion of its life cycle.[9] Although *P. falciparum* has a complex biochemistry and life cycle, recent research has produced a number of potential new therapies.[4,10] Current drug therapies for malaria include quinolines related to chloroquine,[11−13] artemisinins and related dispirotetraoxanes,[14−23] and miscellaneous agents such as febrifugine analogues[24] and atovaquone and proguanil.[25,26] The treatment of malaria has recently been reviewed.[27,28]

Examination of differences in the regulation of gene products between host, vector, and parasite has resulted in identification of target sites or alterations in biochemical regulation, and a number of new targets for drug design have emerged.[29−32] The aspartyl proteases plasmepsin I (Plm I[a]) and plasmepsin II (Plm II) are hemoglobin-degrading aspartyl proteases that have received considerable attention as promising targets for the design of antimalarial agents.[33−35] Four aspartic proteases, Plm I, Plm II, plasmepsin IV (Plm IV), and histoaspartyl protease (HAP) are found in the food vacuole of the parasite and efficiently degrade 75% of host hemoglobin (Figure 1). Plm I and Plm II make the first strategic cleavage of hemoglobin between Phe33 and Leu34 of the α-chain, resulting in protein unfolding and release of the heme moiety.[36−39] Subsequent degradation steps are catalyzed by the cysteine protease falcipain, the metalloprotease falcilysin, and cytoplasmic aminopeptidases (Figure 1).

Plm II is the most thoroughly studied enzyme among the aspartyl proteases of *Plasmodium*. It is made up of 329 amino acids folded into two topologically similar N- and C-terminal domains. The binding cleft contains Asp34 and Asp214, which together represent the catalytic dyad.[40] The catalytic mechanism of plasmepsin II is shown in Figure 2.[41,42] The

*To whom correspondence should be addressed. Phone: 313-577-1523. Fax: 313-577-2033. E-mail: pwoster@wayne.edu.

[a] Abbreviations: Plm I, plasmepsin I; Plm II, plasmepsin II; Plm IV, plasmepsin IV; HAP, histoaspartyl protease; API, aspartyl protease inhibitors; EDC, 1-ethyl-3-(3-dimethylaminopropyl)carbodiimide; HOBT, 1-hydroxybenzotriazole; SDS−PAGE, sodium dodecyl sulfate polyacrylamide gel electrophoreisis; FRET, fluorescence resonance energy transfer; EDANS, 5-[(2-aminoethyl)amino]naphthalene-1-sulfonic acid; DABCYL, 4-(dimethylaminoazo)benzene-4-carboxylic acid; hCatD, human cathepsin D; CHO, Chinese hamster ovary; SOC, super optimal broth with catabolite repression; IPTG, isopropyl β-D-1-thiogalactopyranoside; TB, terrific broth; LB, lysogeny broth; DMEM, Dulbecco's modified Eagle's medium; MES, 2-(*N*-morpholino)ethanesulfonic acid.

 Published on Web 05/03/2010

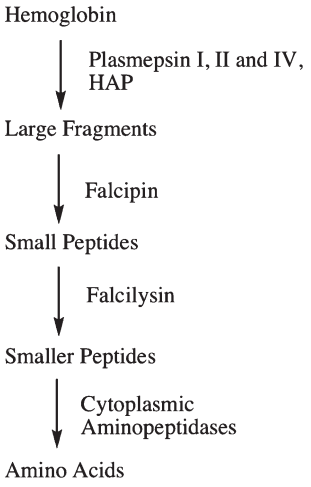

Figure 1. Degradation of hemoglobin by plasmepsins and associated proteases.

Asp34 and Asp214 residues coordinate a water molecule that, following abstraction of a proton by Asp214, attacks the Phe33−Leu34 peptide bond. Hydrolysis of the C−N bond in the transition state then affords two peptides and regenerates the aspartates in the catalytic dyad. As products leave the active site, Asp34 and Asp214 again coordinate a water molecule.

There are numerous examples of aspartyl protease inhibitors (APIs), such as the HIV protease inhibitors saquinavir, ritonavir, indinavir, nelfinavir, lopinavir, and amprenavir,[43−48] that have become effective therapeutic agents, and validated aspartyl protease drug targets include renin, cathepsin D, HIV protease, and β-secretase. A key structural feature in APIs is the presence of a hydroxyl or hydroxyl-like moiety that coordinates to the catalytic dyad, as well as a nonhydrolyzable peptide bond mimic. A number of APIs, including the general aspartyl protease inhibitor pepstatin A, contain a statin core, which serves as a transition state mimic for pepide bond hydrolysis.[49−54] Other transition state analogue cores have been developed for use in constructing APIs,[53,55−57] the most important of which is the hydroxyethylamine core that has been used extensively in HIV protease inhibitors.[58] Pepstatin A coordinates with Asp-34 and Asp-214 in the active site of Plm II (Figure 3) and contains P_1, P_2, P_3, P_1' and P_2' side chain residues that complement the corresponding binding pockets S_1, S_2, etc. Thus, pepstatin A has served as lead compound in the design of various APIs,[59] and pepstatin A analogues such as **2**−**5** (Figure 3) represent reversible inhibitors that are selective for the plasmepsins. The phenylalanine−statin analogue **2** has potent inhibitory activity (K_i = 0.56 nM) with 38-fold selectivity over cathepsin D.[40] It also exhibits activity in cell culture assays, inhibiting growth of cultured *P. falciparum* by 54% at 20 μM. The hydroxyethylene analogue **3** exhibits a K_i of 357 nM against Plm II and 10-fold selectivity over cathepsin D, while hydroxyethylamine analogue **4** exhibits an IC_{50} value of 121 nM against Plm II and completely suppresses parasite growth at 5 μM, with an ED_{50} of 1.6 μM, in an infected erythrocyte assay.[60,61]

All of the reversible Plm II inhibitors described above undergo noncovalent interactions with the enzyme. Mechanism-based or enzyme-activated inhibitors have been reported for various peptidases,[62−64] including a number of serine and cysteine proteases.[65,66] However, reports of irreversible inhibitors of aspartyl proteases are rare,[67,68] and no mechanism-based,

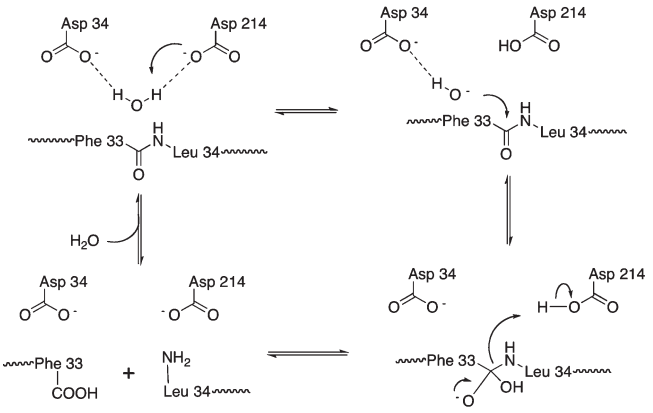

Figure 2. Catalytic mechanism for Plm II-mediated hydrolysis of hemoglobin.

enzyme-activated inactivators for any aspartyl protease have been fully characterized (one report alludes to mechanism-based inhibitors of cathepsin D, but these analogues were never characterized[69]). It has been demonstrated that transition state analogues containing an (*S*)-hydroxyl group displace the enzyme-bound water molecule from the Plm II active site and hydrogen-bond to the catalytic Asp-32 and Asp-214 groups.[70,71] It follows that a peptidomimetic analogue containing an (*S*)-hydroxyl substituent core and bearing a latent electrophile should act as an enzyme-activated, irreversible inhibitor of Plm II. We chose compound **2** and the close homologue TIT1330 (**5**, Figure 3, K_i = 0.5 nM)[72,73] as a starting point for the design of related analogues containing latent electrophilic groups. Putative Plm II inactivators **6**−**9** and their proposed mechanism of inactivation are shown in Figure 4. We reasoned that **6**−**9** would bind to Plm II and coordinate to the catalytic dyad, as described above, followed by activation of the latent electrophilic species.

During activation, we hypothesized that Asp-214 or an adjacent basic amino acid could abstract an acidic proton from the latent electrophile, resulting in the generation of an α,β-unsaturated Michael acceptor (**6**), a ketenimine (**7**), or an allene (**8** and **9**) in the active site (Figure 4). β-Chloroalanine has been used as a mechanism-based inhibitor for pyridoxal phosphate-containing enzymes,[74] and the chloromethyl moiety has been shown to be activated by elimination of HCl both enzymatically[74] and chemically.[75−77] Activation by this route is further supported by the observation that we were unable to isolate the β-fluoro derivative analogous to **6** because of rapid elimination to the corresponding dehydroalanine (see below). The propargyl[78−80] and cyanomethyl[81,82] moieties have been used in the design of mechanism-based inhibitors for various enzymes, although these groups are generally directly appended to a nitrogen or sulfur. These moieties have been shown to be activated by enzymes to the corresponding allene or ketenimine, respectively. In the case of **9**, which contains an *N*-propargyl latent electrophile, this is very likely to occur. However, because the cyanomethyl and propargyl groups of **7** and **8**, respectively, are one carbon removed from an amide nitrogen (thus raising the pK_a of the methylene protons), this is somewhat less likely, although neighboring group assistance from the carbonyl oxygen could facilitate this reaction. A second less likely possibility for the activation of **7** and **8** is the intramolecular formation of a five-membered ring[83] (Figure 4) that could form a covalent bond with an enzyme-bound nucleophile via ring-opening. Following the activation

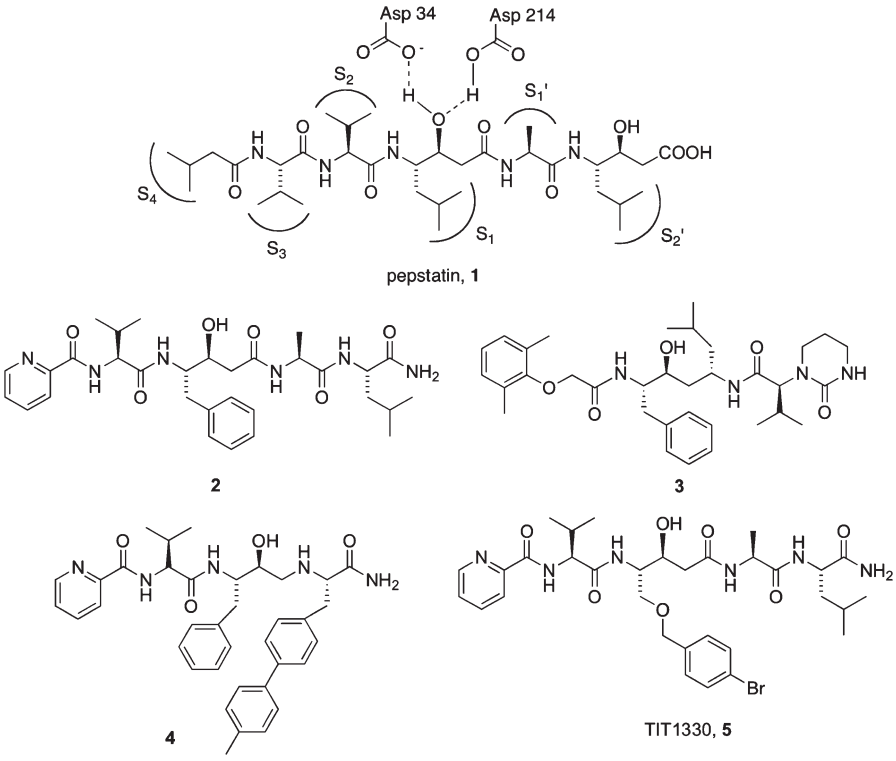

Figure 3. Representation of pepstatin **1** bound in the active site of Plm II, and the structures of Plm II inhibitors **2**–**5**.

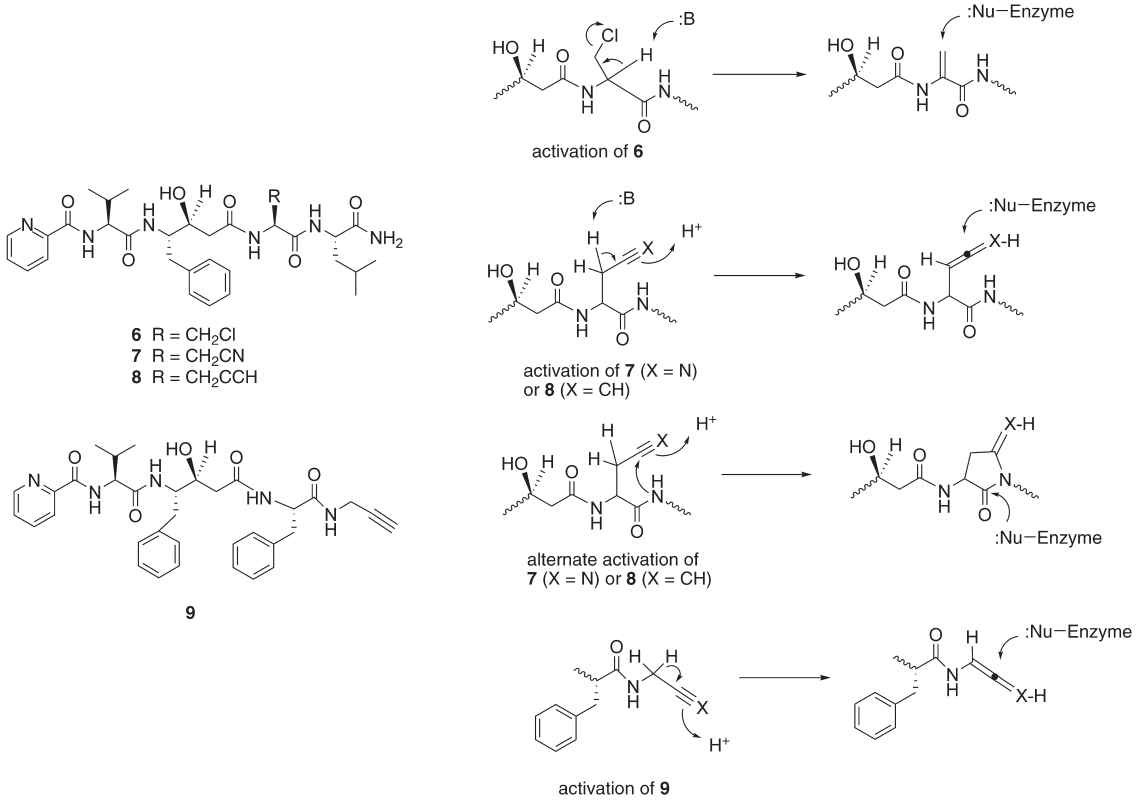

Figure 4. Structures and proposed enzyme-mediated activation of compounds **6**–**9**.

of **6**–**9** as described above, inactivation of the enzyme would then occur when a nucleophilic amino acid residue on the protein formed a covalent bond, forming an irreversible enzyme–inhibitor complex. The parasite must then synthesize new enzyme over an extended period, preventing the degradation of hemoglobin and effectively starving the parasite. Such analogues would have a longer duration of action when compared to reversible inhibitors. Ideally, these agents will be specific for the parasitic target enzyme and thus produce less toxicity in the host cell.[84] The proposed analogues, as well

Scheme 1

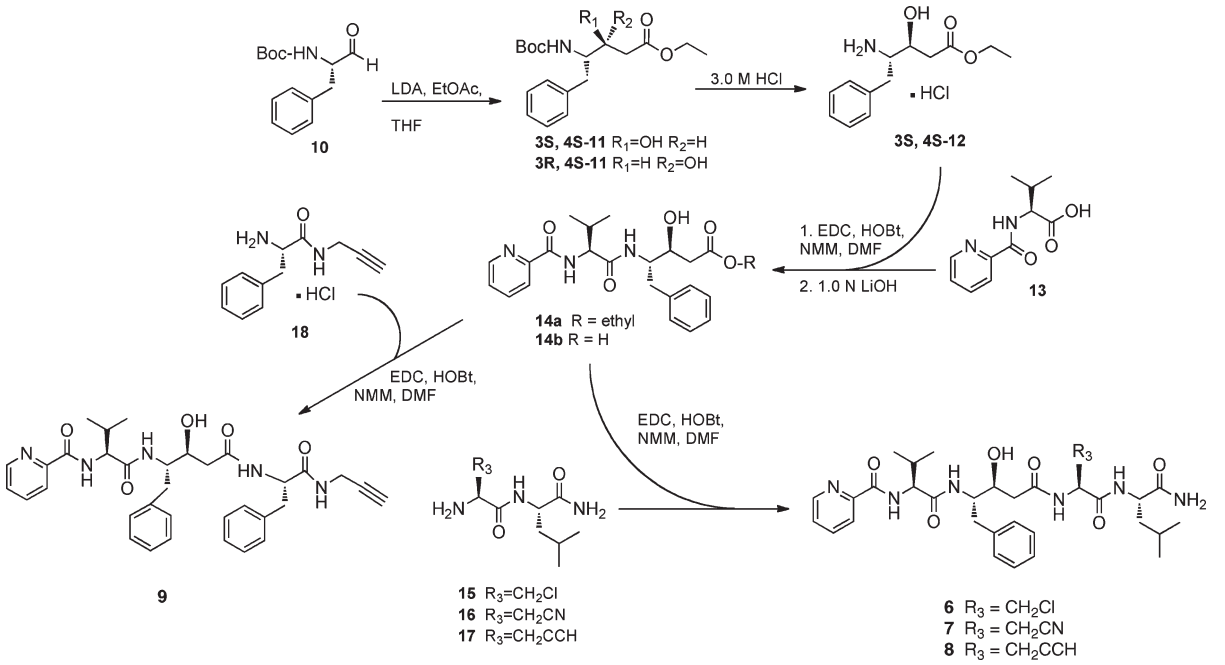

as the methods used to synthesize and evaluate them as Plm II inhibitors, appear in the following sections.

Chemistry

The synthesis of target analogues **6**−**9** is outlined in Scheme 1. *N*-Boc-(*S*)-phenylalanal **10** (synthesized in two steps from (*S*)-phenylalanine methyl ester)[85] was reacted with ethyl acetate (LDA, dry EtOAc/THF) to form the statin precursor **11** as a mixture of the (3*S*,4*S*)- and (3*R*,4*S*)-diastereomers, and the *N*-Boc protecting group was removed (3.0 M HCl) to afford **12** as a mixture of diastereomers. The diastereomers were separated by flash chromatography to afford the pure diastereomers, and their absolute stereochemistry was verified by NMR and polarimetry.[86−88] The synthesis was continued with (3*S*,4*S*)-**12**, which was coupled to intermediate **13** under peptide coupling conditions (EDC, HOBT) to afford the ethyl ester **14a**, followed by ester hydrolysis (1.0 N LiOH) to yield **14b**.[89,90] Dipeptides **15**, **16**, and **17** were synthesized by coupling (*S*)-leucinamide with the commercially available (*S*)-β-chloroalanine, (*S*)-β-cyanoalanine, or (*S*)-α-propargylglycine using the method described above. Attempts to synthesize the (*S*)-β-fluoroalanine-containing dipeptide failed because of rapid elimination to the dehydroalanine derivative during the reaction. Subsequently, compound **14b** was coupled to synthon **15**, **16**, or **17** to form the desired target molecule **6**, **7**, or **8**, respectively. Likewise, coupling of compound **14b** to secondary amine **18** afforded target molecule **9**.[88,89,91,92]

Enzyme Kinetic Studies

Plm II expression and purification was accomplished using published protocols.[93−95] An expression construct encoding the pro form of Plm II was obtained (Dr. Daniel Goldberg, Washington University, St. Louis, MO), verified by DNA sequencing, and used to generate mature Plm II (m-Plm II). The m-Plm II pro form contains an Arg238 codon in place of Lys238,[96] a point mutation that does not affect the kinetic behavior of the enzyme. *Escherichia coli* BL21(DE3) was used to express the pET-3d expression construct of m-Plm II, and a plasmid/cell ratio of 1:20 was used in transfection, according to the standard protocol.[97] Cells were grown overnight in TB media (Terrific Broth, Qbiogene, CA) containing 0.1 mg/mL ampicillin. Induction conditions were optimized in terms of temperature (20 °C/37 °C), media (LB/TB), and IPTG (isopropyl 1-thio-β-D-galactopyranoside, 100−1000 μM). The transfected cells were lysed by passing through a French press followed by sonicating twice for 45 s. Proteins were harvested by centrifugation at 8000*g*, and several rounds of suspension and centrifugation in a range of buffers were necessary to isolate the pure protein fraction, as outlined in the published protocol. For each buffer, the supernatant was collected and analyzed by SDS−PAGE electrophoriesis. Inclusion bodies in the supernatant containing Plm II were solublized and purified by FPLC (heparin FF and Q-Seph columns), and the pure protein fraction was collected and concentrated. The m-Plm II protein was allowed to refold (as verified by non-denaturing gels) and was activated by stirring in sodium citrate buffer, pH 4.7, at a final concentration of 0.1 M. Final purification of m-Plm II was accomplished on a Supradex 100 column, followed by SDS−PAGE analysis. The final purified protein was concentrated and stored at 4 °C in buffer (20 mM Tris-HCl, pH 8.5, 0.25 M NaCl).

Enzyme assays and time dependent kinetics for target compounds **6**−**9** were conducted using a high-throughput FRET-based fluorimetric assay.[60,95,98−100] Analogues were evaluated on the basis of hydrolysis kinetics.[99] Each reaction was initiated by the addition of the substrate DABCYL-Glu-Arg-Nle-Phe-Leu-Ser-Phe-Pro-EDANS, which mimics the Hb-α Phe33-Leu34 initial cleavage site.[101] The fluorophore EDANS is quenched by DABCYL in the intact peptide and expressed following enzymatic cleavage. Assays were performed in NaOAc buffer, pH 5.0, at 37 °C at a final concentration of 2.5 nM enzyme and 1 μM substrate. Inhibitor, enzyme, and substrate were incubated for 30 min at 37 °C, and fluorescence was measured on a photoluminescence fluorimeter (Perkin-Elmer LS-55, excitation wavelength 336 nm, slit width 5 nM; emission wavelength 490 nm, slit width 10 nM). The percentage of inhibition for each sample was calculated on

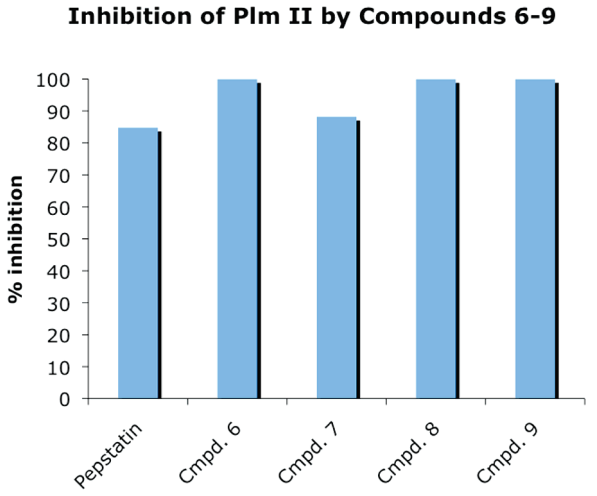

Figure 5. Inhibition of Plm II by compounds **6**–**9** at 1.0 μM. Each data point is the average of three determinations that differed by < 5% in each case.

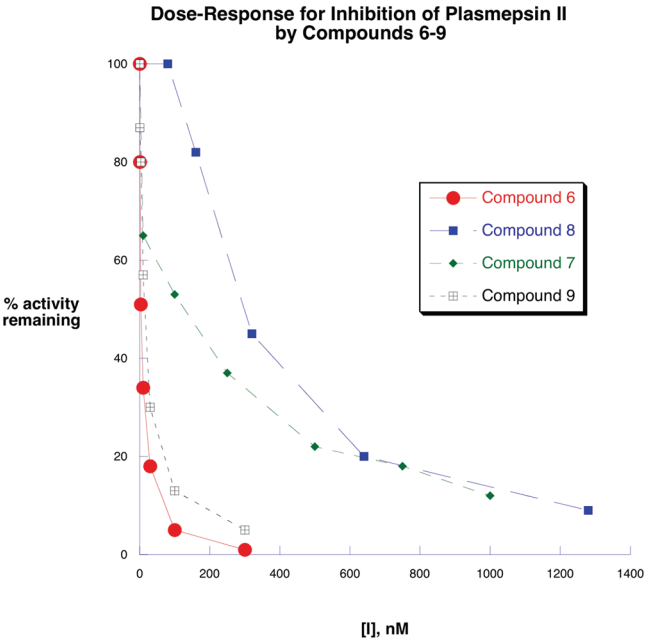

Figure 6. Dose–response curves for the inhibition of PlmII by **6**–**9**. Each data point is the result of three determinations that in each case differed by 5% or less.

the basis of the equation % inhibition = 100 × {1 − [(fluorescence at [I])/(fluorescence of control)]}. Compounds were initially tested at 1 μM, and active compounds were subjected to a dose–response analysis to find exact IC_{50} values. Compounds **6**, **8**, and **9** completely inhibited Plm II at 1.0 μM, while compound **7** produced 88.2% inhibition (Figure 5). All four analogues produced inhibition comparable to pepstatin at the same concentration (82.8% inhibition). Dose–response curves were then generated for **6**–**9** (Figure 6) by assuming competitive inhibition, and IC_{50} values were determined using Kaleidagraph 3.6 (Synergy Software) (compound **6**, 28 nM; compound **7**, 141 nM; compound **8**, 333 nM; compound **9**, 22 nM). Compounds **6** and **8** were selected for further analysis and were subjected to time-dependence studies.[102,103] The reduction of enzyme activity was measured over a 30 min period at 0, 25, 50, 75, and 100 nM inhibitor (Figure 7). A k_{obs} value was derived from each line, and the data were replotted according to the method of Kitz and Wilson,[104] revealing that compound **6** has a K_i value of 35.7 nM and a k_{inact} of 0.025 per min for Plm II. A partition ratio of 84 and a turnover number of 85 were calculated from the corresponding plot of % activity remaining vs [I]/[E]. A similar analysis for compound **8** (Figure 7) revealed the following kinetic constants: K_i = 333.3 nM; k_{inact} = 0.191 per min; partition ratio 98; turnover number 99. Interestingly, although compounds **7** and **9** were both potent inhibitors of Plm II, and both featured potentially activatable electrophiles, neither exhibited time-dependent, pseudo-first-order inhibition kinetics (data not shown).

Dialysis experiments were performed to determine whether compounds **6**–**9** were irreversibly bound to the enzyme or whether dialysis resulted in regeneration of enzyme activity.[102,103,105] For each assay, a fixed amount of enzyme and inhibitor in 500 μL of buffer was incubated at 37 °C for 1–2 h, and residual activity was measured using a 50 μL aliquot. The remaining portion was dialyzed overnight at room temperature in sodium acetate buffer at pH 5.0 containing 10% glycerol and 0.01% Tween-20. Compounds **6**–**9** (1 μM) reduced enzyme activity by 76.9–93.2% under the assay conditions described above, while pepstatin produced a 97.8% inhibition at the same concentration. Following dialysis, enzyme activity was restored to 85.2% and 88.0% for pepstatin and **7**, respectively, and to 36.1% for compound **9**, compared to control However, there was no significant restoration of activity in the cases of **6** and **8** (Figure 8), suggesting that **6** and **8** were covalently bound to the enzyme. These data are consistent with the time-dependent loss of activity observed following treatment with **6** and **8** but not with **7** and **9**. A substrate protection experiment was then employed to demonstrate that **6** and **8** are active-site directed inactivators, as shown in Figure 9. As the ratio of inhibitor to substrate concentration increased, the inactivation of Plm II also increased in a roughly linear fashion, suggesting that the observed time-dependent inactivation is mediated at the active site.

Selectivity and in Vitro Antimalarial Activity

The selectivity of compounds **6**–**9** for Plm II was determined by evaluating these analogues as inhibitors of human cathepsin D (hCatD).[60,95,98] The results of these studies are shown in Figure 10. The IC_{50} values for **6**–**9** against hCatD were determined by assessing percent activity remaining over a range of concentrations (50–2000 nM) using the assay described above (data not shown). The hCatD IC_{50} values for compounds **6**–**9** were then compared to the corresponding values for Plm II as determined above. Compound **8** did not exhibit any selectivity for hCatD of Plm II. However, compounds **6**, **7**, and **9** were found to possess 3.3-, 1.4-, and 10.6-fold selectivity for Plm II. The cytotoxicity of the target molecules in mammalian cells was measured in cultured Chinese hamster ovary (CHO) cells at an inhibitor concentration of 10 μM.[106] As seen in Figure 11, none of the target analogues **6**–**9** produced significant toxicity in the CHO cell line compared to control or DMSO-treated cells. Compound **6** was further tested at 100 and 250 μg/mL and was found to be nontoxic even at these elevated concentrations. These data suggest that compounds **6**–**9** are nontoxic to uninfected mammalian cells.

The antiparasitic activity of **6**, **8**, and **9** was determined in an infected erythrocyte model conducted as previously described.[107,108] A culture of *Plasmodium falciparum* (clone

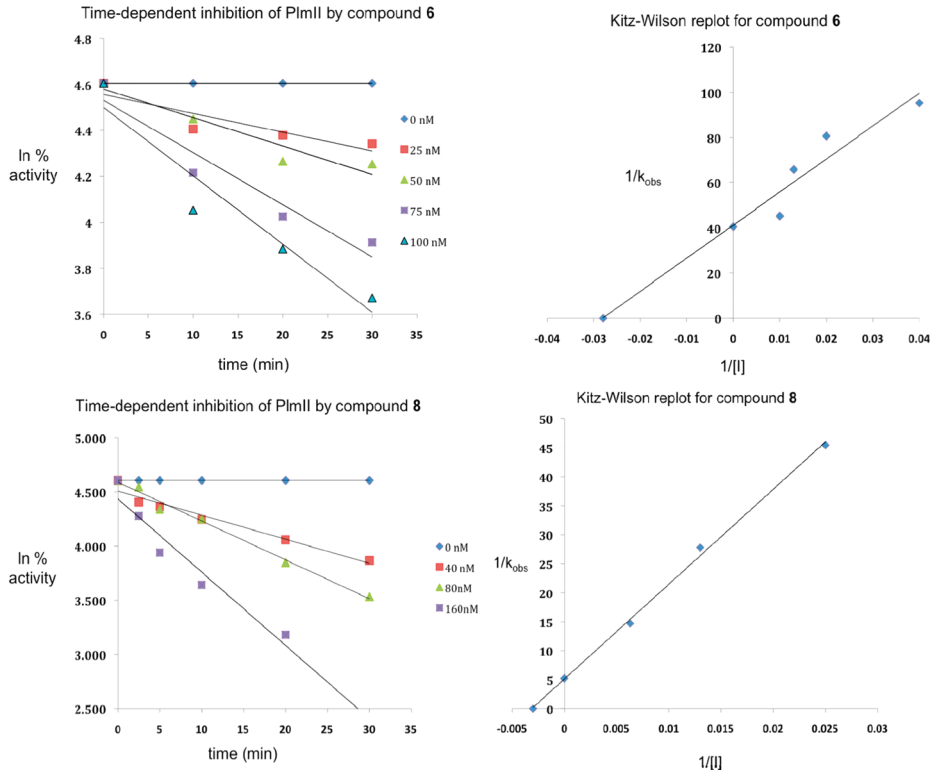

Figure 7. Time-dependent inactivation of Plm II by **6** and **8** and the corresponding Kitz−Wilson replots. Each data point in the time-dependence assay is the average of three determinations that differed by 5% or less in all cases.

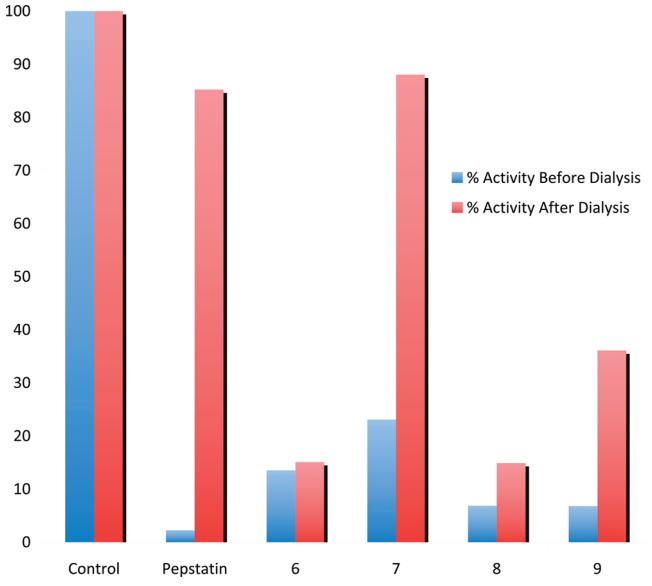

Figure 8. Plm II activity following treatment with 1 μM pepstatin or **6**−**9** before and after dialysis. Each data point is the average of three determinations that differed by 5% or less in all cases.

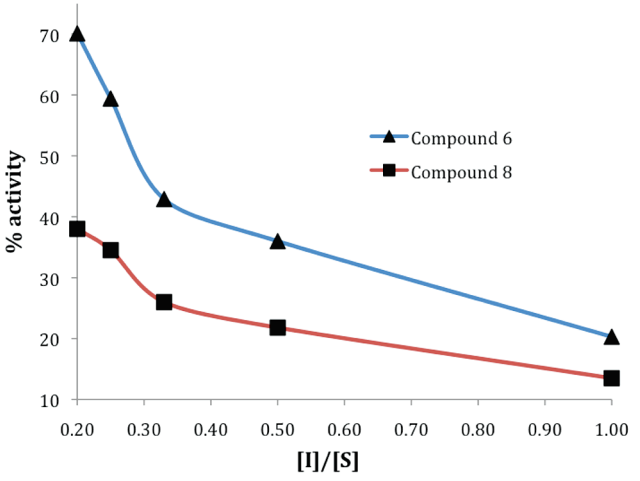

Figure 9. Substrate protection of Plm II from inactivation by **6** and **8**. Plm II was incubated with increasing [I]/[S] at constant [E] for 2 h before measuring activity. Each data point is the average of three determinations that differed by 5% or less in all cases.

3D7) at 2% parasitemia in red blood cells was incubated with various concentrations of inhibitor. This treatment was followed by addition of 1 μCi (17.2 Ci/mmol) of [^{3}H]hypoxanthine, a nucleic acid precursor required for parasite growth. Parasites were harvested, and the cells were isolated by filtration. The amount of radioactive hypoxanthine taken up by the cells was determined by scintillation counting of the dry filters. Parasitemia in the cultures is directly proportional to hypoxanthine incorporation. The IC_{50} value for each of the three inhibitors was calculated from the plot shown in Figure 12. Compound **6** had unremarkable activity, while compounds **8** and **9** exhibited IC_{50} values of 7.7 and 9.2 μM, respectively.

In preliminary molecular modeling studies, the binding of compound **6** Plm II was simulated using the MOE-Dock 2004.03 software docking program. The X-ray coordinates for compound **5** bound to PlmII were obtained from the Protein Data Bank (1W6H.pdb).[73] The structure of the ligand was altered to produce a model of ligand **6**, and the enzyme−inhibitor complex was reminimized. Conformational searching was conducted using simulated annealing (a global optimization technique based on the Monte Carlo method) and

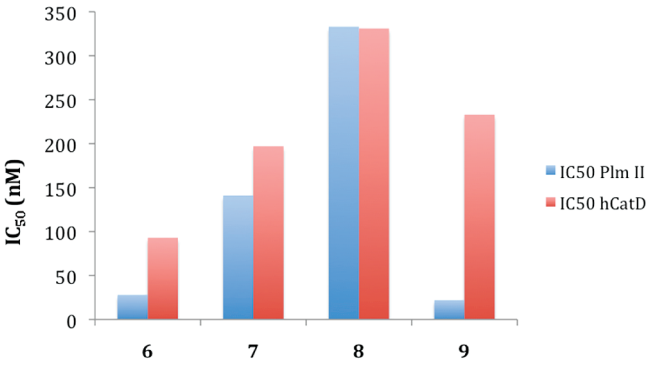

Figure 10. Selectivity between hCatD and Plm II based on IC_{50} values for **6**–**9**.

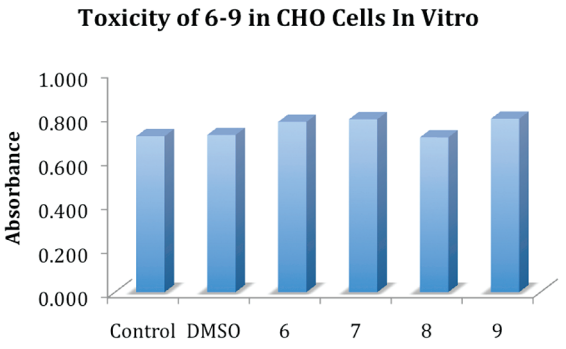

Figure 11. Cytotoxicity of compounds **6**–**9** in cultured CHO cells. Each data point is the average of three determinations that differed by 5% or less in all cases.

the molecular mechanics force field MMFF94. A total of 25 runs were completed, with 6 cycles per run and an 8000 iteration limit, and a 1000 K temperature was maintained during the first cycle. During energy minimization, the chirality of **6** was constrained, and a proximity radius of 7.5 was set. As shown in Figure 13, the (*S*)-hydroxyl group is complexed to both Asp34 and Asp214 at distances of 2.4 and 2.6 Å, respectively. In this orientation, there are a number of nucleophilic residues in proximity to the latent electrophilic chloromethyl moiety present in **6** that could react with an enzyme-generated Michael acceptor, including Tyr77 (3.7 Å), Ser37 (3.5 Å), Thr217 (3.7 Å), and Tyr192 (3.4 Å). The specific amino acid residues involved in the covalent binding of **6** to Plm II will be determined by X-ray crystallographic studies and reported in a subsequent publication.

Discussion

Taken together, the results of the time dependence, dialysis, and substrate protection studies strongly suggest that compounds **6** and **8** represent the first examples of mechanism-based, enzyme-activated inactivators for any aspartyl protease. A similar case could be made for compound **9**, since extensive dialysis resulted in only a 30% increase in Plm II activity following inhibition. However, kinetic analysis did not reveal why compound **7** did not appear to produce inactivation (as evidenced by a nearly complete return of enzyme activity following dialysis). This behavior could potentially be attributed to significantly slower activation of the cyanomethylene latent electrophile by Plm II. Until a crystal structure of the inhibitor/Plm II adducts can be solved, we will not be sure of the mechanism of activation of **6**, **8**, and **9**, and these experiments are now being attempted.

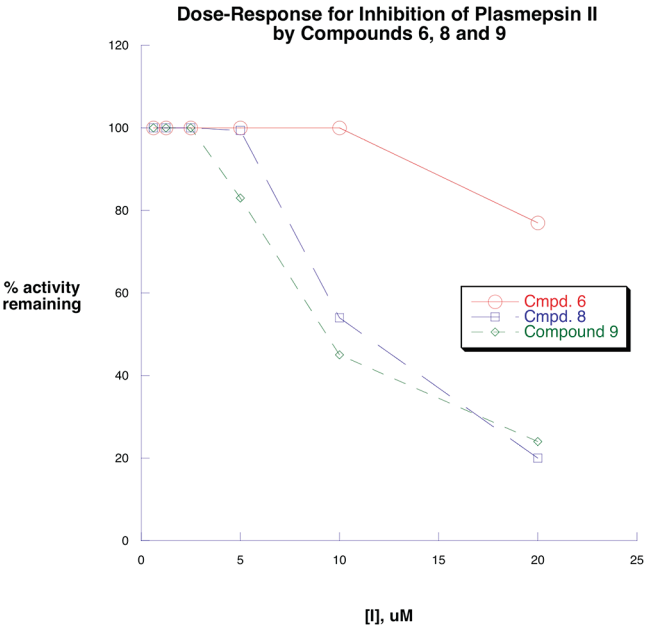

Figure 12. Dose–response curves for compounds **6**, **8**, and **9** against erythrocytes infected with 3D7 *P. falciparum*. Each data point is the average of three determinations that differed by 5% or less in all cases.

Compounds **6** and **8** (K_i of 35.7 and 333.3 nM, respectively) were significantly less potent inhibitors of Plm II than the parent compounds **2** (K_i = 0.56 nM) and **5** (K_i = 0.5 nM), but their K_i values were still found to be in the nanomolar range. Compounds **6** and **8** also possessed reasonable partition ratio values (84 and 98, respectively), indicating they were modestly efficient inactivators. Unfortunately, addition of the latent electrophilic group to **2** and **5** resulted in a significant loss of hCadD/Plm II specificity. Of the analogues where the electrophile was placed adjacent to the statin core, only compound **6** showed a modest preference for Plm II (3.3-fold preference), compared to a 38-fold selectivity for compound **2**.[40] Interestingly, the compound with the greatest selectivity for Plm II, **9**, exhibited a 10.6-fold selectivity for Plm II, despite the fact that the propargyl latent electrophile was located in a terminal position at P_2' rather than adjacent to the transition state core. This value is comparable to the 10-fold selectivity observed for **3**.[60]

As was mentioned above, compound **6** was a poor inhibitor of parasitic growth in vitro, while compounds **8** and **9** exhibited IC_{50} values of 7.7 and 9.2 μM, respectively, in the infected erythrocyte assay. These values are in the same range as the IC_{50} values of 5–20 μM for parent compounds **2**–**5**. These data imply that peptidomimetic inhibitors of Plm II that contain activatable groups retain their in vitro activity against *Plasmodium*, and this observation encourages the synthesis of additional analogues in an effort to improve selectivity between hCatD and Plm II. Recent studies involving a Plm knockout mutant *Plasmodium* strain demonstrate that the parasite produces redundant proteolytic enzymes to ensure an adequate supply of amino acids, and this suggests that additional targets may be involved in the antimalarial activity of peptidomimetics designed to target Plm II.[109] Studies involving previously reported reversible Plm II inhibitors with antimalarial activity suggest that these inhibitors do appear to act on multiple targets.[110] Because Plm II inhibitors **8** and **9** retain the in vitro antimalarial activity observed with reversible Plm II inhibitors, it is reasonable to assume that **8** and **9**

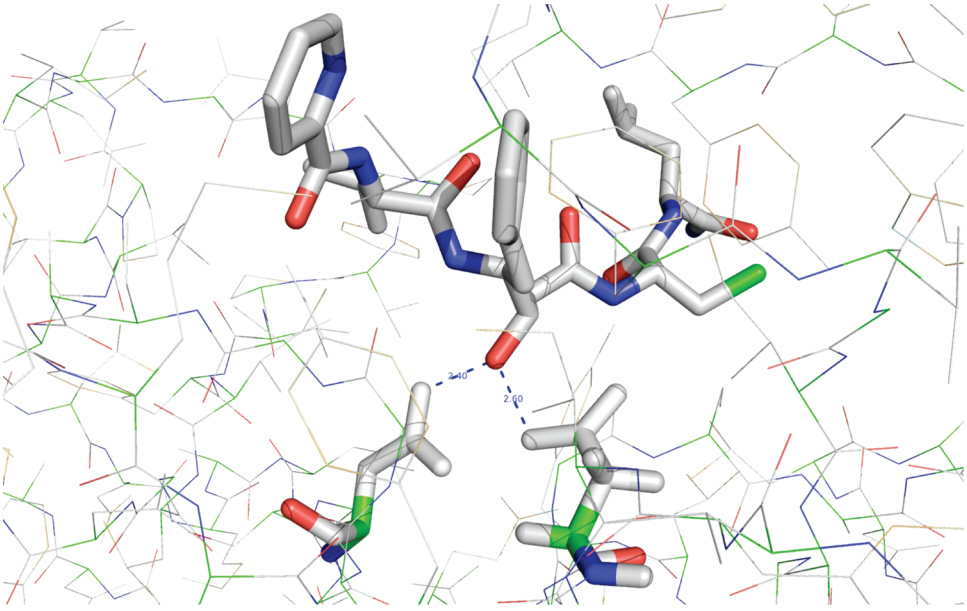

Figure 13. Representation of the transition state mimic hydroxyl of compound **6** coordinated to Asp34 (left) and Asp214 (right) in the active site of Plm II.4.

may also interact with multiple targets. This possibility will be explored as part of our ongoing antimalarial research efforts. In addition, the synthesis of additional compounds in this series and crystallography studies to determine the mechanism of activation of **6** and **8** and the specific amino acid residues involved in covalent bond formation are ongoing concerns in our laboratory.

Experimental Section

General Methods. All reagents were purchased from Sigma/Aldrich Chemical (Milwaukee, WI), Acros Chemical (Chicago, IL), or Bachem (Torrence, CA) and were used without further purification except as noted below. Triethylamine was distilled from potassium hydroxide and stored in a nitrogen atmosphere. Methanol was distilled from magnesium and iodine under a nitrogen atmosphere and stored over molecular sieves. Methylene chloride was distilled from phosphorus pentoxide, and chloroform was distilled from calcium sulfate. Tetrahydrofuran was purified by distillation from sodium and benzophenone. Dimethylformamide was dried by distillation from anhydrous calcium sulfate and was stored under nitrogen. Preparative scale chromatographic procedures were carried out using E. Merck silica gel 60, 230−440 mesh. Thin-layer chromatography was conducted on Merck precoated silica gel 60 F-254. Ion exchange chromatography was conducted on a Dowex 1X8-200 anion-exchange resin. Compound **10** was synthesized from (*S*)-phenylalanine methyl ester as previously described,[85] and compound **13** was synthesized from picolinic acid and (*S*)-valine *tert*-butyl ester as previously reported.[72] Compound (*S*)-**18** was synthesized from (*S*)-phenylalanine and *N*-propargylamine as previously described.[111]

All ^{1}H, ^{13}C and ^{19}F and NMR spectra were recorded on a Varian Mercury 400 MHz or Bruker 300 MHz spectrometer, and all chemical shifts are reported as δ values referenced to TMS or DSS. Infrared spectra were recorded on a Nicolet 5DXB FT-IR spectrophotometer and are referenced to polystyrene. In all cases, ^{1}H NMR, ^{13}C NMR, and IR spectra were consistent with assigned structures. Melting points were recorded on a Thomas-Hoover capillary melting point apparatus and are uncorrected. Mass spectra were recorded on a Kratos MS 80 RFA (EI and CI) or Kratos MS 50 TC (FAB) mass spectrometers. Prior to biological testing, target molecules **6**−**9** were determined to be 95% pure or greater by HPLC chromatography using an Agilent series 1100 high-performance liquid chromatograph fitted with a C18 reversed-phase column.

(3*S*,4*S*)-Ethyl 4-(*tert*-Butoxycarbonylamino)-3-hydroxy-5-phenylpentanoate ((3*S*,4*S*)-11). A solution of 2.46 g of lithium diisopropylamide (0.023 mol, 11.5 mL of a 2.0 M solution in THF/hexane/ethylbenzene) was cooled to −78 °C, and 2.02 g of anhydrous ethyl acetate (0.023 mol, 2.25 mL) in 10 mL of anhydrous THF was added via syringe. The mixture was allowed to stir for 15 min, after which a 2.26 g portion of **10** (0.009 mol) in 20 mL of THF was slowly added. The mixture was then stirred for 10 min, warmed to 0 °C, and acidified to pH 3 with 1 N HCl. The resulting two-phase mixture was washed with three 50 mL portions of ethyl acetate, and the organic layer was washed with brine and dried over anhydrous magnesium sulfate. The mixture was filtered and the solvent removed in vacuo to yield crude **11** as a mixture of the (3*S*,4*S*)- and (3*R*,4*S*)-diastereomers. The diastereomers were then separated by chromatography on silica gel, eluting with 9:1 benzene/ethyl acetate. The desired (3*S*,4*S*)-diastereomer of **11** was isolated as a light-yellow solid (0.576 g, 19.0%). ^{1}H NMR (400 MHz, $CDCl_3$) δ 1.24 (t, J = 6.8 Hz, 3H), 1.35 (s, 9H), 2.34−2.39 (m, 1H), 2.55−2.62 (m, 1H), 2.91 (d, J = 7.6 Hz, 2H), 3.47 (d, J = 2.4 Hz, 1H), 3.73 (q, J = 8.4 Hz, 1H), 3.97−3.99 (m, 1H), 4.13 (q, J = 6.8 Hz, 2H), 4.93 (d, J = 9.6 Hz, 1H), 7.19−7.36 (m, 5H). ^{13}C NMR (100 MHz, $CDCl_3$) δ 14.4, 25.6, 28.5, 36.0, 38.4, 45.0, 50.9, 52.5, 61.0, 61.7, 70.4, 74.4, 86.3, 126.7, 128.7, 161.8, 167.1, 172.3, 173.4. IR (KBr, cm^{-1}) 3352.5, 2981.9, 2936.2, 1733.2, 1681.9, 1525.1, 1368.1, 1314.6, 1168.1, 1031.1. $(M + H)^+$ 283.2. Mp 87 °C. $[\alpha]_D^{20}$ −36.3 (*c* 1.0, MeOH). A 1.19 g portion of the corresponding (3*R*,4*S*)-diastereomer (39.2%) was also isolated as a light-yellow solid. ^{1}H NMR (400 MHz, $CDCl_3$) δ 1.24 (t, J = 6.8 Hz, 3H), 1.41 (br s, 9H), 2.37 (dd, J = 2.4, 21.2 Hz, 1H), 2.58 (dd, J = 10.4, 15.2 Hz, 1H), 2.91 (d, J = 7.6 Hz, 2H), 3.47 (d, J = 2.4 Hz, 1H), 3.72 (q, J = 8.4 Hz, 1H), 3.96−3.99 (m, 1H), 4.13 (q, J = 6.8 Hz, 2H), 4.93 (d, J = 9.6 Hz, 1H, NH), 7.19−7.36 (m, 5H). ^{13}C NMR (100 MHz, $CDCl_3$) δ 14.3, 27.6, 28.5, 38.4, 45.0, 52.5, 70.4, 126.7, 128.7, 167.1, 172.3. Mp 130 °C. $[\alpha]_D^{20}$ +31.4 (*c* 1.0, MeOH).

(3*S*,4*S*)-Ethyl 3-Hydroxy-4-amino-5-phenylpentanoate ((3*S*,4*S*)-12). To a stirring solution of 0.11 g (0.0003 mol) of (3*S*,4*S*)-**11** in 15 mL of ethyl acetate was added 3.0 mL of 3.0 M HCl, and the resulting mixture was allowed to stir at room temperature for 30−40 min. After completion of reaction was

verified by thin-layer chromatography (ethyl acetate/benzene, 1:4), the solvents were removed in vacuo and the resulting solid was triturated with three 20 mL portions of ethyl ether. The combined ether layers were dried (anhydrous $MgSO_4$) to afford (3*S*,4*S*)-**12** (0.066 g, 91.7%). This solid was used without further purification in the subsequent reaction.

Ethyl (3*S*,4*S*)-3-Hydroxy-4-[(*R*)-3-methyl-2-(picolinamido)-butanamido]-5-phenylpentanoic Acid (14a). A 3.6 g (0.016 mol) portion of **13** was dissolved in 25 mL of anhydrous DMF at 0 °C, and 2.48 g of 1-ethyl-3-(3-dimethylaminopropyl)carbodiimide (EDC) (0.016 mol) and 2.16 g of hydroxybenzotriazole (HOBT) (0.016 mol) were added. The mixture was allowed to stir for 15 min at 0 °C. Then 1.62 g (1.78 mL, 0.0160 mol) of *N*-methylmorpholine was added, and the resulting mixture was stirred for another 15 min at 0 °C. A 4.38 g (0.016 mol) portion of (3*S*,4*S*)-**12** dissolved in 15 mL of anhydrous DMF was then added to the reaction mixture, which was stirred for 8 h at room temperature. Removal of the solvent under reduced pressure yielded a dark-yellow semisolid. The semisolid was dissolved in water and extracted with three 50 mL portions of chloroform, the combined organic layers were dried over anhydrous magnesium sulfate and filtered, and the solvent was removed to afford the crude ethyl ester of **14**. This intermediate was purified on silica gel to yield 5.39 g of the pure ethyl ester of **14** (76.3%). ^{1}H NMR (400 MHz, $CDCl_3$) δ 0.87−1.05 (m, 6H), 1.24 (t, J = 7.2 Hz, 3H), 2.17−2.35 (m, 1H), 2.38, 2.43 (dd, J = 2.8 Hz, 2.8 Hz, 1H), 2.52, 2.56 (dd, J = 10.0 Hz, 10.0 Hz, 1H), 2.88−2.96 (m, 2H), 3.78 (m, 1H), 4.1 (q, J = 6.4 Hz, 2H), 4.40, 4.42 (dd, J = 6.4 Hz, 2.8 Hz, 1H), 6.23 (s, 1H, OH), 7.04−7.24 (m, 4H), 7.41−7.48 (m, 1H), 7.57 (dt, J = 8 Hz, 0.8 Hz, 1H), 7.68 (d, J = 8.4 Hz, 1H), 7.87 (dt, J = 7.6 Hz, 1.6 Hz, 1H), 8.04 (d, J = 8.4 Hz, 1H, NH), 8.18 (d, J = 8.0 Hz 1H), 8.43 (d, J = 9.2 Hz, 1H, NH), 8.59 (d, J = 4.4 Hz, 1H). ^{13}C NMR (100 MHz, $CDCl_3$) δ 14.3, 17.98, 19.84, 30.61, 38.42, 39.07, 54.25, 59.32, 61.08, 67.47, 85.30, 109.62, 120.41, 122.59, 125.27, 126.56, 126.67, 128.61, 128.74, 128.88, 129.0, 129.54, 137.58, 138.03, 148.52, 149.48, 164.87, 171.09, 173.42. IR (KBr, cm^{-1}) 3333.8, 2962.3, 1732.2, 1651.4, 1521.3, 1434.5, 1260.7, 1153.0, 1087.7.

(3*S*,4*S*)-3-Hydroxy-4-[(*R*)-3-methyl-2-(picolinamido)butanamido]-5-phenylpentanoic Acid (14b). A 5.39 g (0.012 mol) portion of the ethyl ester of **14a** was dissolved in 25 mL of dioxane/water (4:2) and cooled to 0 °C, and 20 mL of 2.0 N NaOH was added to the mixture by dropwise addition. The solution was warmed to room temperature and allowed to stir for 16 h, during which time the reaction was monitored by TLC. The mixture was again cooled to 0 °C and neutralized by the dropwise addition of 1.0 N HCl. The resultant solution was washed with two 25 mL portions of diethyl ether (2×), and the aqueous layer was extracted with three 50 mL portions of ethyl acetate. The ethyl acetate layers were combined, washed with brine, and dried over anhydrous magnesium sulfate. Removal of the solvent in vacuo yielded compound (3*S*,4*S*)-**14b** as a light-brown hygroscopic solid (4.70 g, 94.7%) of sufficient purity to be used in the next reaction. ^{1}H NMR (400 MHz, $CDCl_3$) δ 0.71−0.91 (m, 6H), 2.29 (d, J = 7.2 Hz, 1H), 2.55−2.57 (m, 1H), 2.59−2.61 (m, 1H), 2.74−2.85 (m, 1H), 2.98−3.06 (m, 1H), 3.71 (m, 1H, OH), 4.05−4.15 (m, 1H), 4.20−4.36 (m, 1H), 7.06−7.22 (m, 3H), 7.43−7.52 (m, 2H), 7.76−7.92 (m, 2H), 8.55−8.62 (m, 2H). ^{13}C NMR (100 MHz, $CDCl_3$) δ 14.41, 19.34, 21.28, 38.47, 59.43, 60.66, 126.47, 126.72, 128.51, 128.71, 129.47, 137.93, 148.95, 171.33, 175.63. IR (KBr, cm^{-1}) 3316.7, 3059.2, 2964.9, 2927.5, 1715.2, 1651.8, 1525.3, 1434.7, 1259.2, 1096.2, 914.3.

(*S*)-2-[(*R*)-2-Amino-3-chloropropanamido]-4-methylpentanamide (15). A 2.0 g (0.016 mol) portion of 2-amino-3-chloropropanoic acid was dissolved in 30 mL of anhydrous DMF, and the solution was cooled to 0 °C in an ice bath. To this mixture was added 1-ethyl-3-(3-dimethylaminopropyl)carbodiimide (EDC, 3.72 g, 0.020 mol) and 1-hydroxybenzotriazole (HOBt, 2.6 g, 0.020 mol), and the mixture was allowed to stir for 15 min at 0 °C. After 15 min 2.02 g (0.020 mol, 2.2 mL) of *N*-methylmorpholine was added and the mixture was stirred for another 15 min at 0 °C. A 2.6 g (0.020 mol) portion of (*S*)-leucinamide dissolved in 5 mL of DMF was then added by syringe, and the mixture was warmed to room temperature and allowed to stir for 8 h at room temperature. The solvent was then removed under high vacuum to yield a dark-yellow semisolid. The semisolid was dissolved in 50 mL of water and extracted with three 50 mL portions of chloroform. The combined organic layers were dried over anhydrous magnesium sulfate and filtered, and the solvent was removed to afford crude **15**, which was purified by column chromatography to afford 2.92 g of pure **15** as a pale-yellow oil (77.5% yield). ^{1}H NMR (400 MHz, $CDCl_3$) δ 0.81−0.86 (m, 6H), 1.47−1.57 (m, 3H), 3.66 (dd, J = 5.2 Hz, 1H), 3.79 (d, J = 4.8 Hz, 1H), 4.33−4.36 (m, 2H). ^{13}C NMR (100 MHz, $CDCl_3$) δ 25.72, 26.96, 44.99, 52.41, 53.26, 53.68, 59.59, 172.50, 213.21.

(*S*)-2-[(*S*)-2-Amino-3-cyanopropanamido]-4-methylpentanamide (16). Compound **16** was synthesized from 2-aminopent-4-ynoic acid and (*S*)-leucinamide exactly as described for the synthesis of **15** in 83.7% yield. ^{1}H NMR (400 MHz, $CDCl_3$) δ 0.93−0.99 (m, 6H), 1.60−1.74 (m, 3H), 2.76 (dd, J = 8.8 and 9.2 Hz, 1H), 2.96 (dd, J = 4.0 and 4.4 Hz, 1H), 4.18−4.24 (m, 1H), 4.19−4.48 (m, 1H). ^{13}C NMR (100 MHz, $CDCl_3$) δ 25.55, 28.68, 52.45, 52.88, 53.09, 53.52, 59.37, 137.68, 170.99, 175.47.

(*S*)-2-Amino-*N*-[(*S*)-1-amino-4-methyl-1-oxopentan-2-yl]pent-4-ynamide (17). Compound **17** was synthesized from 2-amino-3-cyanopropanoic acid and (*S*)-leucinamide exactly as described for the synthesis of **15** in 74.2% yield. ^{1}H NMR (400 MHz, $CDCl_3$) δ 0.88−0.94 (m, 6H), 1.56−1.58 (m, 1H), 1.65−1.75 (m, 2H), 2.61−2.96 (m, 2H), 2.88 (s, 1H), 4.31 (br s, 1H), 4.50−4.56 (m, 1H), 5.48 (d, J = 6.4 Hz, 1H), 6.00 (br s, 1H), 6.70 (br s, 1H), 7.08 (d, J = 7.6 Hz, 1H). ^{13}C NMR (100 MHz, $CDCl_3$) δ 20.71, 22.03, 23.68, 27.24, 39.67, 50.48, 52.22, 70.96, 78.15, 169.54, 173.52.

***N*-((*S*)-1-(((2*S*,3*S*)-5-(((*R*)-1-(((*S*)-1-Amino-4-methyl-1-oxopentan-2-yl)amino)-3-chloro-1-oxopropan-2-yl)amino)-3-hydroxy-5-oxo-1-phenylpentan-2-yl)amino)-3-methyl-1-oxobutan-2-yl)picolinamide (6).** Compound **6** was prepared from **14b** and **15** using the peptide coupling method described for the synthesis of **15** and was isolated as a light-yellow solid in 25.5% yield. ^{1}H NMR (100 MHz, $CDCl_3$) δ 0.81−0.99 (m, 12H), 1.60−1.76 (m, 3H), 2.24−2.43 (m, 2H), 2.58 (d, J = 8.0 Hz, 1H), 2.85−3.06 (m, 2H), 3.49 (s, 1H, OH), 3.65−3.93 (m, 2H), 4.04−4.68 (m, 5H), 7.13−7.25 (m, 3H), 7.39−7.52 (m, 2H), 7.83−7.90 (m, 1H), 8.08−8.17 (m, 1H), 8.42−8.51 (m, 1H), 8.58−8.62 (m, 1H). ^{13}C NMR (100 MHz, $CDCl_3$) δ 9.95, 13.04, 21.96, 22.72, 27.90, 28.68, 29.33, 30.27, 37.7, 39.9, 44.8, 50.34, 67.14, 84.07, 108.40, 119.17, 124.05, 127.78, 129.88, 131.43, 166.77. MS ESI+ 631.5 ($M + H^+$).

***N*-((*S*)-1-(((2*S*,3*S*)-5-(((*S*)-1-(((*S*)-1-Amino-4-methyl-1-oxopentan-2-yl)amino)-1-oxopent-4-yn-2-yl)amino)-3-hydroxy-5-oxo-1-phenylpentan-2-yl)amino)-3-methyl-1-oxobutan-2-yl)picolinamide (7).** Compound **7** was prepared from **14b** and **16** using the peptide coupling method described for the synthesis of **15** and was isolated as a white solid in 24.1% yield. ^{1}H NMR (400 MHz, $CDCl_3$) δ 0.77−1.01 (m, 12H), 1.25−1.34 (m, 3H), 2.16−2.48 (m, 3H), 2.85−3.03 (m, 4H), 4.03−4.17 (m, 4H), 4.32−4.44 (m, 2H), 7.12−7.26 (m, 3H), 7.40−7.52 (m, 2H), 7.88 (m, 2H, 1H = NH), 8.11−8.19 (m, 2H, 1H = NH), 8.38−8.42 (m, 1H), 8.42−8.60 (m, 2H, 1H = NH). ^{13}C NMR (100 MHz, $CDCl_3$) δ 16.36, 28.68, 63.76, 65.71, 84.06, 93.63, 108.41, 110.29, 119.20, 124.04, 127.77, 136.01, 147.38, 151.49, 166.38, 180.68, 202.12, 208.63. MS (*m*/*e*) ESI+ 660.4 ($M^+ + K$).

***N*-((*S*)-1-(((2*S*,3*S*)-5-(((*S*)-1-(((*S*)-1-Amino-4-methyl-1-oxopentan-2-yl)amino)-3-cyano-1-oxopropan-2-yl)amino)-3-hydroxy-5-oxo-1-phenylpentan-2-yl)amino)-3-methyl-1-oxobutan-2-yl)picolinamide (8).** Compound **8** was prepared from **14b** and **17** using the peptide coupling method described for the synthesis of **15** and was isolated as a white solid in 18.6% yield. ^{1}H NMR (400 MHz, $CDCl_3$) δ 0.67−0.90 (m, 12H), 1.50−1.17 (m, 3H), 2.33−2.42 (m, 2H), 2.53−2.97 (m, 6H), 4.08−4.56 (m, 6H), 7.06−7.24 (m, 4H),

7.41−7.52 (m, 1H), 7.84−7.91 (m, 1H), 8.11−8.21 (m, 1H), 8.26 (d, J = 8.0 Hz, 1H, NH), 8.43 (dd, J = 6.8 Hz, 6.4 Hz, 1H), 8.56 (d, J = 4.4 Hz, 1H), 8.61 (d, J = 4.4 Hz, 1H). ^{13}C NMR (100 MHz, $CDCl_3$) δ 18.6, 21.4, 24.9, 29.9, 31.7, 46.7, 54.4, 66.1, 70.6, 92.5, 97.7, 112.7, 122.3, 123.0, 128.8, 129.4, 152.6, 162.9, 173.7, 174.9, 181.9, 191.4. MS ESI+ 643.3 ($M + Na^+$).

***N*-((*S*)-1-(((2*S*,3*S*)-3-Hydroxy-5-oxo-5-(((*S*)-1-oxo-3-phenyl-1-(prop-2-yn-1-ylamino)propan-2-yl)amino)-1-phenylpentan-2-yl)-amino)-3-methyl-1-oxobutan-2-yl)picolinamide (9).** Compound **9** was prepared from **14b** and **18** using the peptide coupling method described for the synthesis of **15** and was isolated as a white solid in 22.1% yield. ^{1}H NMR (400 MHz, $CDCl_3$) δ 0.73−1.11 (m, 6H), 1.98−2.70 (m, 4H), 2.78−2.82 (m, 1H), 2.94−3.48 (m, 3H), 3.72−4.31 (m, 5H), 4.72−5.30 (m, 1H), 7.14−7.31 (m, 8H), 7.41−7.53 (m, 1H), 7.84−7.89 (m, 2H), 8.07−8.31 (m, 1H), 8.46−8.61 (m, 2H). ^{13}C NMR (100 MHz, $CDCl_3$) δ 19.44, 19.65, 28.68, 53.52, 89.64, 90.08, 93.76, 106.61, 111.67, 116.13, 121.35, 127.42, 128.28, 145.18, 147.39, 158.65, 159.01, 165.19, 181.17, 183.67, 190.91, 198.29. MS ESI+ 598.3 ($M + H^+$).

Plasmepsin II Expression and Purification. Competent BL21-DE3 cells were thawed on ice and gently mixed, and an amount of 100 μL of these cells was added to 15 mL of prechilled Falcon 2059 culture tubes and kept on ice. Then 2.5 μL of a 1.0 M stock 2-mercaptoethanol solution was added to each culture tube and kept on ice for 10 min, with gentle swirling every 2 min. This step was followed by the addition of 1, 2, and 3 μL of plasmid to corresponding tubes. For the positive control transformation reaction, 1 μL of the pUC18 control plasmid (empty vector) was added to a separate 100 μL aliquot of the competent cells and swirled gently. A negative control of BL-21CE-3 cells without any transformation was included. Cells were incubated on ice for 30 min, after which super optimal broth with catabolite repression (SOC) medium was preheated to 42 °C, and the cells were heat-shocked for 45 s in water bath and returned to ice for 2 min. A 900 μL portion of SOC medium (42 °C) was added to each culture, and cells were incubated at 37 °C for 1 h with shaking at 225−270 rpm. After 1 h, 100 μL of the cell culture was plated on LB agar plates containing 100 mg/mL ampicillin and incubated overnight at 37 °C. An isolated colony on agar plate was chosen and put into 2 mL of LB media containing 1% ampicillin, and this sample plus an identical duplicate was agitated in a cell shaker at 220 rpm (37 °C) overnight. The next morning, 50 μL of each culture was pipetted into fresh 1 mL aliquots of LB broth containing no ampicillin and reincubated at 37 °C for 2 h with shaking at 220 rpm. The culture was split into two 2 mL samples, one of which was used for induction and the second as control. Induction was started by adding isopropyl β-D-1-thiogalactopyranoside (IPTG) to a final concentration of 1 mM when the optical density was ≥4. These samples were incubated at 220 rpm in a cell shaker at 37 °C until the optical density reached 1.0. Protein expression was then analyzed by SDS−PAGE. Induction conditions were varied in terms of media (LB/TB), temperature (20 °C/37 °C) and IPTG concentration (0.1−1 mM) for optimum expression of the desired protein. Cell cultures were diluted to 1.0 L and centrifuged, and the resulting cell pellet was resuspended in 20 mL of buffer A (20 mM Tris-HCl, pH 8.5, 1 mM EDTA, 150 mM NaCl). The cells were lysed with two passes through a French press and then sonicated two times for 15 s. The resulting mixture was then centrifuged at 15 000 rpm for 20 min, and the supernatant was saved for SDS−PAGE. Cells were again resuspended in buffer A and repelleted. Inclusion bodies were then washed two times each with buffer B (20 mM Tris-HCl, pH 8.5, 1 mM EDTA, 150 mM NaCl, 1% Triton X-100) and then buffer C (20 mM Tris-HCl, pH 8.5, 1 mM EDTA). Inclusion bodies were then solublized in buffer D (6 M urea, 20 mM Tris-HCl, pH 8.5, 1 mM EDTA). The supernatant was dialyzed overnight in buffer D, and the protein solution was filtered through a 45 μm and then a 20 μm filter. The resulting protein solution was then loaded onto a heparin-Sepharose FF column equilibrated in buffer D. Plm II was collected in the flow through and again loaded onto a mono-Q-Sepharose column equilibrated in buffer D. Proteins were eluted from the mono-Q-Sepharose column with a linear gradient of 0−1.0 M NaCl. The eluent was dialyzed in buffer E (20 mM Tris-HCl, pH 8.5, 1 mM EDTA, 10% glycerol) at room temperature while stirring overnight at room temperature. Refolding of the protein was ensured using native gels. The major portion of protein was collected from the heparin FF column by running a 0−1.0 M NaCl gradient. This was again loaded onto a heparin FF column, and a 0−1.0 M NaCl gradient was run. This eluent was again loaded onto a Q-Sephrose column equilibrated with buffer D followed by refolding in buffer E. Autoactivation was then achieved by stirring in 0.1 M sodium citrate solution at pH 4.7. Small molecular fragments were removed by loading them on Q-Sepharose column equilibrated in buffer E, and the column was eluted with a salt gradient (0−1.0 M NaCl). In the final purification step, the resultant eluant was loaded onto a Superdex 100 column using buffer F (20 mM Tris-HCl, pH 8.5, 1 mM EDTA, 10% glycerol, 0.25 M NaCl) and the protein was then stored at 4 °C in buffer G (20 mM 2-(*N*-morpholino)ethanesulfonic acid (MES), pH 6.0, 0.25 M NaCl) and concentrated to give the desired concentration.

Plasmepsin II Inhibition Assay. Enzyme activity was determined on the basis of FRET (fluorescence resonance energy transfer) assays using internally quenched fluorescent peptide substrates. The substrate used was EDANS-CO-CH_2-CH_2-CO-ALERMFLSFP-diaminopimelate-(DABCYL)OH. A Perkin-Elmer LS 55 luminescence spectrophotometer was used for initial assays, followed by quantitation using a SpectraMax M5 microplate reader (Molecular Devices) using an excitation wavelength of 336 nm (slit width 5) and an emission wavelength of 490 nm (slit width 10). Assays were performed in 0.5 M sodium acetate buffer at pH 5.0 containing 10% glycerol and 0.01% Tween-20. Stock solutions in DMSO were diluted to give a final DMSO concentration of 1%. Typically, 2.5 nM enzyme was incubated with different concentrations of each inhibitor to make a final 1 μM concentration of the substrate. Enzyme activity was measured as an increase in fluorescence intensity after a 30 min incubation period. Inhibition was reported as percent inhibition compared to control, and active compounds were further titrated to get initial IC_{50} and K_i values by assuming competitive inhibition. Logarithmic fitting of the data was achieved using the KaleidaGraph graphing software. For time-dependent inactivators, K_i values were derived using the method of Kitz and Wilson.[104]

Time-Dependent Kinetics. Depending upon the IC_{50} value of the analogues, different concentrations of analogues were incubated with a 2.5 nM enzyme concentration so that in the final reaction mixture **6** was present at 0, 25, 50, 75, and 100 nM, while **8** was present at 0, 40, 80, 160, 240, 320 nM. Incubations were conducted for 0, 2.5, 5, 10, 20, 30, 40 min at 37 °C. After each incubation, 10 μL from each reaction mixture was added to a 96-well plate containing 90 μL of substrate (1 μM final concentration). Fluorescence was then measured after 2 min of incubation at 37 °C, and a control sample was used to calculate the percent enzyme activity remaining. These values were converted to ln(percent activity) and plotted against time to give a pseudo-first-order rate constant (k_{obs}) for each concentration of inhibitor. This rate constant was then replotted against the inverse of the inhibitor concentration to derive the kinetic parameters K_i and k_{inact}.

Substrate Protection Experiments. To determine whether increasing substrate concentration protected the enzyme from inactivation by **6** or **8**, inhibitor and substrate were mixed in ratios varying from 1:1 to 1:5 and incubated at a 2.5 nM final concentration of enzyme. Following a 2 min incubation period at 37 °C, fluorescence values were measured and compared to control values.

Dialysis and Spun Column Chromatography. A 300 μL aliquot of Plm II solution (3 nM final concentration) was incubated with 300 μL of inhibitors **6**−**9** (1 μM final concentration) for 1 h to achieve complete inactivation. Enzymes without any inhibitor

or with 1 μM pepstatin-A were used as controls. After 1 h, a 50 μL aliquot was removed and assayed against 50 μL of substrate (final concentration 1 μM) to assess the remaining enzyme activity. The reaction mixture was then transferred to dialysis cassettes (molecular weight cutoff of 10 000 Da) and dialyzed overnight against 0.1 M sodium acetate buffer, pH 5.0, at room temperature. The buffer was changed three times during this period. After overnight dialysis, activity was again measured as described above. Spun chromatography was also utilized to validate the data from the dialysis experiments. In this method, each incubated reaction mixture was loaded onto spin column cartridges according to the manufacturer protocol and centrifuged for 5 min at 1800 rpm at 4 °C. The eluent was then assayed for residual activity.

Cytotoxicity Studies (MTS Assay). CHO cells were used for all cytotoxicity assays. Cells were aspirated from Dulbecco's modified Eagle's medium (DMEM) and rinsed with 10 mL of phosphate buffered saline twice (aspirating each time). A 1.5 mL aliquot of trypsin was added, and the mixture was incubated at 37 °C and 5% CO_2 until cells became detached. Cells were then washed twice with 10 mL of phosphate buffered saline to protect the cells. Stock solutions of inhibitors were prepared and incubated with cells at a final concentration of 10 μM for 24 h at 37 °C and 5.0% CO_2. After 24 h, cells were washed with medium. The MTS reagent was prepared by mixing 20 μL of PMS, 2 mL of MTS, and 0.2 mL of medium. An amount of 20 μL of the reagent was added to each well in the cell plates. Cells were then incubated for 2 h at 37 °C and 5.0% CO_2. The plate was then read with the plate reader set at OD 490. Absorbance values were compared with control to measure cytotoxicity.

Selectivity Assay against hCatD (Human Cathepsin D). A stock solution of human cathepsin D (hCatD, Sigma/Aldrich) was prepared in 0.1 M formic acid buffer (pH 3.7). The activity of hCatD was determined over a range of concentrations of **6**−**9** (50−2000 nM) using the procedure described for the assay of Plm II with enzyme at a 1 nM final concentration. Activity was calculated compared to a control containing no inhibitor. Comparison of the IC_{50} values for each inhibitor against Plm II and hCatD was used to express selectivity.

Infected Erythrocyte Assay. Assays evaluating the effects of compounds on parasite growth were performed using a modification of the [^{3}H]hypoxanthine incorporation assay as described previously.[107,108] Briefly, a highly synchronous culture containing early trophozoite stage parasites (~1% hematocrit and 1% parasitemia) was supplemented with [^{3}H]hypoxanthine to 10 μCi mL^{-1}, and then 50 μL aliquots were transferred into wells of flat-bottomed 96-well microtiter plates. Wells were supplemented with an equal volume of medium containing various concentrations of test compound (1−5 μM final) or DMSO (maximum final concentration 1% v/v). Plates were then transferred to gassed boxes and cultured at 37 °C for 30 h to allow parasite development to the mature schizont stage. Cultures were then harvested onto glass fiber filters using a cell harvester. Filters were wetted with scintillation cocktail, and bound radioactivity was quantified in a β-scintillation counter. Control cultures containing established growth-inhibitory compounds or without parasites were used. The amount of radioactivity in each sample was expressed relative to that in the control wells containing DMSO only. Experiments were performed in triplicate (n = 3), and the experimental values were averaged.

Acknowledgment. We are indebted to Professor Daniel Goldberg, Washington University, St. Louis, MO, for providing the construct for the expression of Plm II and for performing the infected erythrocyte assay experiments.

References

(1) Bowman, S.; Lawson, D.; Basham, D.; Brown, D.; Chillingworth, T.; Churcher, C. M.; Craig, A.; Davies, R. M.; Devlin, K.; Feltwell, T.; Gentles, S.; Gwilliam, R.; Hamlin, N.; Harris, D.; Holroyd, S.; Hornsby, T.; Horrocks, P.; Jagels, K.; Jassal, B.; Kyes, S.; McLean, J.; Moule, S.; Mungall, K.; Murphy, L.; Oliver, K.; Quail, M. A.; Rajandream, M. A.; Rutter, S.; Skelton, J.; Squares, R.; Squares, S.; Sulston, J. E.; Whitehead, S.; Woodward, J. R.; Newbold, C.; Barrell, B. G. The complete nucleotide sequence of chromosome 3 of *Plasmodium falciparum*. *Nature* **1999**, *400* (6744), 532–538.

(2) Morel, C. M. Reaching maturity: 25 years of the TDR. *Parasitol. Today* **2000**, *16* (12), 522–528.

(3) Wahlgren, M.; Bejarano, M. T. A blueprint of "bad air". *Nature* **1999**, *400* (6744), 506–507.

(4) Macreadie, I.; Ginsburg, H.; Sirawaraporn, W.; Tilley, L. Antimalarial drug development and new targets. *Parasitol. Today* **2000**, *16* (10), 438–444.

(5) Whittey, C. J. M.; Rowland, M.; Sanderson, F.; Mutabingwa, T. K. Malaria. *Br. Med. J.* **2002**, *325*, 1221–1224.

(6) Schwobel, B.; Alifrangis, M.; Salanti, A.; Jelinek, T. Different mutation patterns of atovaquone resistance to *Plasmodium falciparum* in vitro and in vivo: rapid detection of codon 268 polymorphisms in the cytochrome *b* as potential in vivo resistance marker. *Malar. J.* **2003**, *2*, 5.

(7) Labbe, A. C.; Bualombai, P.; Pillai, D. R.; Zhong, K. J.; Vanisaveth, V.; Hongvanthong, B.; Looareesuwan, S.; Kain, K. C. Molecular markers for chloroquine-resistant *Plasmodium falciparum* malaria in Thailand and Laos. *Ann. Trop. Med. Parasitol.* **2001**, *95* (8), 781–788.

(8) Valderramos, S. G.; Fidock, D. A. Transporters involved in resistance to antimalarial drugs. *Trends Pharmacol. Sci.* **2006**, *27* (11), 594–601.

(9) Garcia, L. S.; Bruckner, D. A. *Diagnostic Medical Parasitology*; American Society for Microbiology: Washington, DC, 1993.

(10) Nwaka, S.; Hudson, A. Innovative lead discovery strategies for tropical diseases. *Nat. Rev. Drug Discovery* **2006**, *5* (11), 941–955.

(11) Brueckner, R. P.; Coster, T.; Wesche, D. L.; Shmuklarsky, M.; Schuster, B. G. Prophylaxis of *Plasmodium falciparum* infection in a human challenge model with WR 238605, a new 8-aminoquinoline antimalarial. *Antimicrob. Agents Chemother.* **1998**, *42* (5), 1293–1294.

(12) Raynes, K. J.; Stocks, P. A.; O'Neill, P. M.; Park, B. K.; Ward, S. A. New 4-aminoquinoline Mannich base antimalarials. 1. Effect of an alkyl substituent in the 5′-position of the 4′-hydroxyanilino side chain. *J. Med. Chem.* **1999**, *42* (15), 2747–2751.

(13) Stocks, P. A.; Raynes, K. J.; Bray, P. G.; Park, B. K.; O'Neill, P. M.; Ward, S. A. Novel short chain chloroquine analogues retain activity against chloroquine resistant K1 *Plasmodium falciparum*. *J. Med. Chem.* **2002**, *45* (23), 4975–4983.

(14) McCullough, K. J.; Wood, J. K.; Bhattacharjee, A. K.; Dong, Y.; Kyle, D. E.; Milhous, W. K.; Vennerstrom, J. L. Methyl-substituted dispiro-1,2,4,5-tetraoxanes: correlations of structural studies with antimalarial activity. *J. Med. Chem.* **2000**, *43* (6), 1246–1249.

(15) Meshnick, S. R.; Jefford, C. W.; Posner, G. H.; Avery, M. A.; Peters, W. Second-generation antimalarial endoperoxides. *Parasitol. Today* **1996**, *12* (2), 79–82.

(16) O'Neill, P. M.; Miller, A.; Bishop, L. P.; Hindley, S.; Maggs, J. L.; Ward, S. A.; Roberts, S. M.; Scheinmann, F.; Stachulski, A. V.; Posner, G. H.; Park, B. K. Synthesis, antimalarial activity, biomimetic iron(II) chemistry, and in vivo metabolism of novel, potent C-10-phenoxy derivatives of dihydroartemisinin. *J. Med. Chem.* **2001**, *44* (1), 58–68.

(17) O'Neill, P. M.; Scheinmann, F.; Stachulski, A. V.; Maggs, J. L.; Park, B. K. Efficient preparations of the beta-glucuronides of dihydroartemisinin and structural confirmation of the human glucuronide metabolite. *J. Med. Chem.* **2001**, *44* (9), 1467–1470.

(18) Posner, G. H.; Dai, H.; Bull, D. S.; Lee, J. K.; Eydoux, F.; Ishihara, Y.; Welsh, W.; Pryor, N.; Petr, S., Jr. Lewis acid-promoted, stereocontrolled, gram scale, Diels−Alder cycloadditions of electronically matched 2-pyrones and vinyl ethers: the critical importance of molecular sieves and the temperature of titanium coordination with the pyrone. *J. Org. Chem.* **1996**, *61* (2), 671–676.

(19) Posner, G. H.; Parker, M. H.; Northrop, J.; Elias, J. S.; Ploypradith, P.; Xie, S.; Shapiro, T. A. Orally active, hydrolytically stable, semisynthetic, antimalarial trioxanes in the artemisinin family. *J. Med. Chem.* **1999**, *42* (2), 300–304.

(20) Posner, G. H.; Ploypradith, P.; Parker, M. H.; O'Dowd, H.; Woo, S. H.; Northrop, J.; Krasavin, M.; Dolan, P.; Kensler, T. W.; Xie, S.; Shapiro, T. A. Antimalarial, antiproliferative, and antitumor activities of artemisinin-derived, chemically robust, trioxane dimers. *J. Med. Chem.* **1999**, *42* (21), 4275–4280.

(21) Vennerstrom, J. L.; Ager, A. L., Jr.; Andersen, S. L.; Grace, J. M.; Wongpanich, V.; Angerhofer, C. K.; Hu, J. K.; Wesche, D. L.

Assessment of the antimalarial potential of tetraoxane WR 148999. *Am. J. Trop. Med. Hyg.* **2000**, *62* (5), 573–578.
(22) Wu, Y. How might qinghaosu (artemisinin) and related compounds kill the intraerythrocytic malaria parasite? A chemist's view. *Acc. Chem. Res.* **2002**, *35* (5), 255–259.
(23) Kim, H. S.; Begum, K.; Ogura, N.; Wataya, Y.; Nonami, Y.; Ito, T.; Masuyama, A.; Nojima, M.; McCullough, K. J. Antimalarial activity of novel 1,2,5,6-tetraoxacycloalkanes and 1,2,5-trioxacycloalkanes. *J. Med. Chem.* **2003**, *46* (10), 1957–1961.
(24) Kikuchi, H.; Tasaka, H.; Hirai, S.; Takaya, Y.; Iwabuchi, Y.; Ooi, H.; Hatakeyama, S.; Kim, H. S.; Wataya, Y.; Oshima, Y. Potent antimalarial febrifugine analogues against the Plasmodium malaria parasite. *J. Med. Chem.* **2002**, *45* (12), 2563–2570.
(25) Labbe, A. C.; Loutfy, M. R.; Kain, K. C. Recent advances in the prophylaxis and treatment of malaria. *Curr. Infect. Dis. Rep.* **2001**, *3* (1), 68–76.
(26) Woster, P. M. New therapies for malaria. *Annu. Rep. Med. Chem.* **2003**, *38* (21), 203–211.
(27) Daily, J. P. Antimalarial drug therapy: the role of parasite biology and drug resistance. *J. Clin. Pharmacol.* **2006**, *46* (12), 1487–1497.
(28) Winstanley, P.; Ward, S. Malaria chemotherapy. *Adv. Parasitol.* **2006**, *61*, 47–76.
(29) Gardner, M. J.; Hall, N.; Fung, E.; White, O.; Berriman, M.; Hyman, R. W.; Carlton, J. M.; Pain, A.; Nelson, K. E.; Bowman, S.; Paulsen, I. T.; James, K.; Eisen, J. A.; Rutherford, K.; Salzberg, S. L.; Craig, A.; Kyes, S.; Chan, M. S.; Nene, V.; Shallom, S. J.; Suh, B.; Peterson, J.; Angiuoli, S.; Pertea, M.; Allen, J.; Selengut, J.; Haft, D.; Mather, M. W.; Vaidya, A. B.; Martin, D. M.; Fairlamb, A. H.; Fraunholz, M. J.; Roos, D. S.; Ralph, S. A.; McFadden, G. I.; Cummings, L. M.; Subramanian, G. M.; Mungall, C.; Venter, J. C.; Carucci, D. J.; Hoffman, S. L.; Newbold, C.; Davis, R. W.; Fraser, C. M.; Barrell, B. Genome sequence of the human malaria parasite *Plasmodium falciparum*. *Nature* **2002**, *419* (6906), 498–511.
(30) Holt, R. A.; Subramanian, G. M.; Halpern, A.; Sutton, G. G.; Charlab, R.; Nusskern, D. R.; Wincker, P.; Clark, A. G.; Ribeiro, J. M.; Wides, R.; Salzberg, S. L.; Loftus, B.; Yandell, M.; Majoros, W. H.; Rusch, D. B.; Lai, Z.; Kraft, C. L.; Abril, J. F.; Anthouard, V.; Arensburger, P.; Atkinson, P. W.; Baden, H.; de Berardinis, V.; Baldwin, D.; Benes, V.; Biedler, J.; Blass, C.; Bolanos, R.; Boscus, D.; Barnstead, M.; Cai, S.; Center, A.; Chaturverdi, K.; Christophides, G. K.; Chrystal, M. A.; Clamp, M.; Cravchik, A.; Curwen, V.; Dana, A.; Delcher, A.; Dew, I.; Evans, C. A.; Flanigan, M.; Grundschober-Freimoser, A.; Friedli, L.; Gu, Z.; Guan, P.; Guigo, R.; Hillenmeyer, M. E.; Hladun, S. L.; Hogan, J. R.; Hong, Y. S.; Hoover, J.; Jaillon, O.; Ke, Z.; Kodira, C.; Kokoza, E.; Koutsos, A.; Letunic, I.; Levitsky, A.; Liang, Y.; Lin, J. J.; Lobo, N. F.; Lopez, J. R.; Malek, J. A.; McIntosh, T. C.; Meister, S.; Miller, J.; Mobarry, C.; Mongin, E.; Murphy, S. D.; O'Brochta, D. A.; Pfannkoch, C.; Qi, R.; Regier, M. A.; Remington, K.; Shao, H.; Sharakhova, M. V.; Sitter, C. D.; Shetty, J.; Smith, T. J.; Strong, R.; Sun, J.; Thomasova, D.; Ton, L. Q.; Topalis, P.; Tu, Z.; Unger, M. F.; Walenz, B.; Wang, A.; Wang, J.; Wang, M.; Wang, X.; Woodford, K. J.; Wortman, J. R.; Wu, M.; Yao, A.; Zdobnov, E. M.; Zhang, H.; Zhao, Q.; Zhao, S.; Zhu, S. C.; Zhimulev, I.; Coluzzi, M.; della Torre, A.; Roth, C. W.; Louis, C.; Kalush, F.; Mural, R. J.; Myers, E. W.; Adams, M. D.; Smith, H. O.; Broder, S.; Gardner, M. J.; Fraser, C. M.; Birney, E.; Bork, P.; Brey, P. T.; Venter, J. C.; Weissenbach, J.; Kafatos, F. C.; Collins, F. H.; Hoffman, S. L. The genome sequence of the malaria mosquito *Anopheles gambiae*. *Science* **2002**, *298* (5591), 129–149.
(31) Lander, E. S.; Linton, L. M.; Birren, B.; Nusbaum, C.; Zody, M. C.; Baldwin, J.; Devon, K.; Dewar, K.; Doyle, M.; FitzHugh, W.; Funke, R.; Gage, D.; Harris, K.; Heaford, A.; Howland, J.; Kann, L.; Lehoczky, J.; LeVine, R.; McEwan, P.; McKernan, K.; Meldrim, J.; Mesirov, J. P.; Miranda, C.; Morris, W.; Naylor, J.; Raymond, C.; Rosetti, M.; Santos, R.; Sheridan, A.; Sougnez, C.; Stange-Thomann, N.; Stojanovic, N.; Subramanian, A.; Wyman, D.; Rogers, J.; Sulston, J.; Ainscough, R.; Beck, S.; Bentley, D.; Burton, J.; Clee, C.; Carter, N.; Coulson, A.; Deadman, R.; Deloukas, P.; Dunham, A.; Dunham, I.; Durbin, R.; French, L.; Grafham, D.; Gregory, S.; Hubbard, T.; Humphray, S.; Hunt, A.; Jones, M.; Lloyd, C.; McMurray, A.; Matthews, L.; Mercer, S.; Milne, S.; Mullikin, J. C.; Mungall, A.; Plumb, R.; Ross, M.; Shownkeen, R.; Sims, S.; Waterston, R. H.; Wilson, R. K.; Hillier, L. W.; McPherson, J. D.; Marra, M. A.; Mardis, E. R.; Fulton, L. A.; Chinwalla, A. T.; Pepin, K. H.; Gish, W. R.; Chissoe, S. L.; Wendl, M. C.; Delehaunty, K. D.; Miner, T. L.; Delehaunty, A.; Kramer, J. B.; Cook, L. L.; Fulton, R. S.; Johnson, D. L.; Minx, P. J.; Clifton, S. W.; Hawkins, T.; Branscomb, E.; Predki, P.; Richardson, P.; Wenning, S.; Slezak, T.; Doggett, N.; Cheng, J. F.; Olsen, A.; Lucas, S.; Elkin, C.; Uberbacher, E.; Frazier, M.; Gibbs, R. A.; Muzny, D. M.; Scherer, S. E.; Bouck, J. B.; Sodergren, E. J.; Worley, K. C.; Rives, C. M.; Gorrell, J. H.; Metzker, M. L.; Naylor, S. L.; Kucherlapati, R. S.; Nelson, D. L.; Weinstock, G. M.; Sakaki, Y.; Fujiyama, A.; Hattori, M.; Yada, T.; Toyoda, A.; Itoh, T.; Kawagoe, C.; Watanabe, H.; Totoki, Y.; Taylor, T.; Weissenbach, J.; Heilig, R.; Saurin, W.; Artiguenave, F.; Brottier, P.; Bruls, T.; Pelletier, E.; Robert, C.; Wincker, P.; Smith, D. R.; Doucette-Stamm, L.; Rubenfield, M.; Weinstock, K.; Lee, H. M.; Dubois, J.; Rosenthal, A.; Platzer, M.; Nyakatura, G.; Taudien, S.; Rump, A.; Yang, H.; Yu, J.; Wang, J.; Huang, G.; Gu, J.; Hood, L.; Rowen, L.; Madan, A.; Qin, S.; Davis, R. W.; Federspiel, N. A.; Abola, A. P.; Proctor, M. J.; Myers, R. M.; Schmutz, J.; Dickson, M.; Grimwood, J.; Cox, D. R.; Olson, M. V.; Kaul, R.; Raymond, C.; Shimizu, N.; Kawasaki, K.; Minoshima, S.; Evans, G. A.; Athanasiou, M.; Schultz, R.; Roe, B. A.; Chen, F.; Pan, H.; Ramser, J.; Lehrach, H.; Reinhardt, R.; McCombie, W. R.; de la Bastide, M.; Dedhia, N.; Blocker, H.; Hornischer, K.; Nordsiek, G.; Agarwala, R.; Aravind, L.; Bailey, J. A.; Bateman, A.; Batzoglou, S.; Birney, E.; Bork, P.; Brown, D. G.; Burge, C. B.; Cerutti, L.; Chen, H. C.; Church, D.; Clamp, M.; Copley, R. R.; Doerks, T.; Eddy, S. R.; Eichler, E. E.; Furey, T. S.; Galagan, J.; Gilbert, J. G.; Harmon, C.; Hayashizaki, Y.; Haussler, D.; Hermjakob, H.; Hokamp, K.; Jang, W.; Johnson, L. S.; Jones, T. A.; Kasif, S.; Kaspryzk, A.; Kennedy, S.; Kent, W. J.; Kitts, P.; Koonin, E. V.; Korf, I.; Kulp, D.; Lancet, D.; Lowe, T. M.; McLysaght, A.; Mikkelsen, T.; Moran, J. V.; Mulder, N.; Pollara, V. J.; Ponting, C. P.; Schuler, G.; Schultz, J.; Slater, G.; Smit, A. F.; Stupka, E.; Szustakowski, J.; Thierry-Mieg, D.; Thierry-Mieg, J.; Wagner, L.; Wallis, J.; Wheeler, R.; Williams, A.; Wolf, Y. I.; Wolfe, K. H.; Yang, S. P.; Yeh, R. F.; Collins, F.; Guyer, M. S.; Peterson, J.; Felsenfeld, A.; Wetterstrand, K. A.; Patrinos, A.; Morgan, M. J.; de Jong, P.; Catanese, J. J.; Osoegawa, K.; Shizuya, H.; Choi, S.; Chen, Y. J. Initial sequencing and analysis of the human genome. *Nature* **2001**, *409* (6822), 860–921.
(32) Venter, J. C.; Adams, M. D.; Myers, E. W.; Li, P. W.; Mural, R. J.; Sutton, G. G.; Smith, H. O.; Yandell, M.; Evans, C. A.; Holt, R. A.; Gocayne, J. D.; Amanatides, P.; Ballew, R. M.; Huson, D. H.; Wortman, J. R.; Zhang, Q.; Kodira, C. D.; Zheng, X. H.; Chen, L.; Skupski, M.; Subramanian, G.; Thomas, P. D.; Zhang, J.; Gabor Miklos, G. L.; Nelson, C.; Broder, S.; Clark, A. G.; Nadeau, J.; McKusick, V. A.; Zinder, N.; Levine, A. J.; Roberts, R. J.; Simon, M.; Slayman, C.; Hunkapiller, M.; Bolanos, R.; Delcher, A.; Dew, I.; Fasulo, D.; Flanigan, M.; Florea, L.; Halpern, A.; Hannenhalli, S.; Kravitz, S.; Levy, S.; Mobarry, C.; Reinert, K.; Remington, K.; Abu-Threideh, J.; Beasley, E.; Biddick, K.; Bonazzi, V.; Brandon, R.; Cargill, M.; Chandramouliswaran, I.; Charlab, R.; Chaturvedi, K.; Deng, Z.; Di Francesco, V.; Dunn, P.; Eilbeck, K.; Evangelista, C.; Gabrielian, A. E.; Gan, W.; Ge, W.; Gong, F.; Gu, Z.; Guan, P.; Heiman, T. J.; Higgins, M. E.; Ji, R. R.; Ke, Z.; Ketchum, K. A.; Lai, Z.; Lei, Y.; Li, Z.; Li, J.; Liang, Y.; Lin, X.; Lu, F.; Merkulov, G. V.; Milshina, N.; Moore, H. M.; Naik, A. K.; Narayan, V. A.; Neelam, B.; Nusskern, D.; Rusch, D. B.; Salzberg, S.; Shao, W.; Shue, B.; Sun, J.; Wang, Z.; Wang, A.; Wang, X.; Wang, J.; Wei, M.; Wides, R.; Xiao, C.; Yan, C.; Yao, A.; Ye, J.; Zhan, M.; Zhang, W.; Zhang, H.; Zhao, Q.; Zheng, L.; Zhong, F.; Zhong, W.; Zhu, S.; Zhao, S.; Gilbert, D.; Baumhueter, S.; Spier, G.; Carter, C.; Cravchik, A.; Woodage, T.; Ali, F.; An, H.; Awe, A.; Baldwin, D.; Baden, H.; Barnstead, M.; Barrow, I.; Beeson, K.; Busam, D.; Carver, A.; Center, A.; Cheng, M. L.; Curry, L.; Danaher, S.; Davenport, L.; Desilets, R.; Dietz, S.; Dodson, K.; Doup, L.; Ferriera, S.; Garg, N.; Gluecksmann, A.; Hart, B.; Haynes, J.; Haynes, C.; Heiner, C.; Hladun, S.; Hostin, D.; Houck, J.; Howland, T.; Ibegwam, C.; Johnson, J.; Kalush, F.; Kline, L.; Koduru, S.; Love, A.; Mann, F.; May, D.; McCawley, S.; McIntosh, T.; McMullen, I.; Moy, M.; Moy, L.; Murphy, B.; Nelson, K.; Pfannkoch, C.; Pratts, E.; Puri, V.; Qureshi, H.; Reardon, M.; Rodriguez, R.; Rogers, Y. H.; Romblad, D.; Ruhfel, B.; Scott, R.; Sitter, C.; Smallwood, M.; Stewart, E.; Strong, R.; Suh, E.; Thomas, R.; Tint, N. N.; Tse, S.; Vech, C.; Wang, G.; Wetter, J.; Williams, S.; Williams, M.; Windsor, S.; Winn-Deen, E.; Wolfe, K.; Zaveri, J.; Zaveri, K.; Abril, J. F.; Guigo, R.; Campbell, M. J.; Sjolander, K. V.; Karlak, B.; Kejariwal, A.; Mi, H.; Lazareva, B.; Hatton, T.; Narechania, A.; Diemer, K.; Muruganujan, A.; Guo, N.; Sato, S.; Bafna, V.; Istrail, S.; Lippert, R.; Schwartz, R.; Walenz, B.; Yooseph, S.; Allen, D.; Basu, A.; Baxendale, J.; Blick, L.; Caminha, M.; Carnes-Stine, J.; Caulk, P.; Chiang, Y. H.; Coyne, M.; Dahlke, C.; Mays, A.; Dombroski, M.; Donnelly, M.; Ely, D.; Esparham, S.; Fosler, C.; Gire, H.; Glanowski, S.; Glasser, K.; Glodek, A.; Gorokhov, M.; Graham, K.; Gropman, B.; Harris, M.; Heil, J.; Henderson, S.; Hoover, J.; Jennings, D.; Jordan, C.; Jordan, J.; Kasha, J.; Kagan, L.; Kraft, C.; Levitsky, A.; Lewis, M.; Liu, X.; Lopez, J.; Ma, D.; Majoros, W.; McDaniel, J.; Murphy, S.;

Newman, M.; Nguyen, T.; Nguyen, N.; Nodell, M.; Pan, S.; Peck, J.; Peterson, M.; Rowe, W.; Sanders, R.; Scott, J.; Simpson, M.; Smith, T.; Sprague, A.; Stockwell, T.; Turner, R.; Venter, E.; Wang, M.; Wen, M.; Wu, D.; Wu, M.; Xia, A.; Zandieh, A.; Zhu, X. The sequence of the human genome. *Science* **2001**, *291* (5507), 1304–1351.

(33) Coombs, G. H.; Goldberg, D. E.; Klemba, M.; Berry, C.; Kay, J.; Mottram, J. C. Aspartic proteases of *Plasmodium falciparum* and other parasitic protozoa as drug targets. *Trends Parasitol.* **2001**, *17* (11), 532–537.

(34) Francis, S. E.; Sullivan, D. J., Jr.; Goldberg, D. E. Hemoglobin metabolism in the malaria parasite *Plasmodium falciparum*. *Annu. Rev. Microbiol.* **1997**, *51*, 97–123.

(35) Rosenthal, P. J.; Meshnick, S. R. Hemoglobin catabolism and iron utilization by malaria parasites. *Mol. Biochem. Parasitol.* **1996**, *83* (2), 131–139.

(36) Banerjee, R.; Liu, J.; Beatty, W.; Pelosof, L.; Klemba, M.; Goldberg, D. E. Four plasmepsins are active in the *Plasmodium falciparum* food vacuole, including a protease with an active-site histidine. *Proc. Natl. Acad. Sci. U.S.A.* **2002**, *99* (2), 990–995.

(37) Goldberg, D. E. Hemoglobin degradation. *Curr. Top. Microbiol. Immunol.* **2005**, *295*, 275–291.

(38) Goldberg, D. E. S.; A, F. G.; Beavis, R.; Chait, B.; Cerami, A.; Henderson, G. B. Hemoglobin degradation in the human malaria pathogen *Plasmodium falciparum*: a catabolic pathway initiated by a specific aspartic protease. *J. Exp. Med.* **1991**, *173*, 961–969.

(39) Klemba, M.; Goldberg, D. E. Biological roles of proteases in parasitic protozoa. *Annu. Rev. Biochem.* **2002**, *71*, 275–305.

(40) Silva, A. M.; Lee, A. Y.; Gulnik, S. V.; Maier, P.; Collins, J.; Bhat, T. N.; Collins, P. J.; Cachau, R. E.; Luker, K. E.; Gluzman, I. Y.; Francis, S. E.; Oksman, A.; Goldberg, D. E.; Erickson, J. W. Structure and inhibition of plasmepsin II, a hemoglobin-degrading enzyme from *Plasmodium falciparum*. *Proc. Natl. Acad. Sci. U.S.A.* **1996**, *93* (19), 10034–10039.

(41) Bjelic, S.; Aqvist, J. Computational prediction of structure, substrate binding mode, mechanism, and rate for a malaria protease with a novel type of active site. *Biochemistry* **2004**, *43* (46), 14521–14528.

(42) Northrop, D. B. Follow the protons: a low-barrier hydrogen bond unifies the mechanisms of the aspartic proteases. *Acc. Chem. Res.* **2001**, *34* (10), 790–797.

(43) Kempf, D. J.; Marsh, K. C.; Kumar, G.; Rodrigues, A. D.; Denissen, J. F.; McDonald, E.; Kukulka, M. J.; Hsu, A.; Granneman, G. R.; Baroldi, P. A.; Sun, E.; Pizzuti, D.; Plattner, J. J.; Norbeck, D. W.; Leonard, J. M. Pharmacokinetic enhancement of inhibitors of the human immunodeficiency virus protease by coadministration with ritonavir. *Antimicrob. Agents Chemother.* **1997**, *41* (3), 654–660.

(44) Lacy, M. K.; Abriola, K. P. Indinavir: a pharmacologic and clinical review of a new HIV protease inhibitor. *Conn. Med.* **1996**, *60* (12), 723–727.

(45) Pakyz, A.; Israel, D. Overview of protease inhibitors. *J. Am. Pharm. Assoc.* **1997**, *NS37* (5), 543–551.

(46) Patick, A. K.; Potts, K. E. Protease inhibitors as antiviral agents. *Clin. Microbiol. Rev.* **1998**, *11* (4), 614–627.

(47) Shetty, B. V.; Kosa, M. B.; Khalil, D. A.; Webber, S. Preclinical pharmacokinetics and distribution to tissue of AG1343, an inhibitor of human immunodeficiency virus type 1 protease. *Antimicrob. Agents Chemother.* **1996**, *40* (1), 110–114.

(48) Adkins, J. C.; Faulds, D. Amprenavir. *Drugs* **1998**, *55* (6), 837–842; discussion 843−834 .

(49) Kunimoto, S.; Aoyagi, T.; Morishima, H.; Takeuchi, T.; Umezawa, H. Mechanism of inhibition of pepsin by pepstatin. *J. Antibiot.* (*Tokyo*) **1972**, *25* (4), 251–255.

(50) Marciniszyn, J., Jr.; Hartsuck, J. A.; Tang, J. Mode of inhibition of acid proteases by pepstatin. *J. Biol. Chem.* **1976**, *251* (22), 7088–7094.

(51) Marshall, G. R. Structure−activity relations of antagonists of the renin−angiotensin system. *Fed. Proc.* **1976**, *35* (13), 2494–2501.

(52) Rich, D. H. Pepstatin-derived inhibitors of aspartic proteinases. A close look at an apparent transition-state analogue inhibitor. *J. Med. Chem.* **1985**, *28* (3), 263–273.

(53) Rich, D. H. In *Comprehensive Medicinal Chemistry: The Rational Design, Mechanistic Study and Therapeutic Applications of Chemical Compounds*; Hansch, C., Sammes, P. G., Taylor, J. B., Eds; Pergamon Press: New York, 1990; Vol. 2, pp 391−441.

(54) Umezawa, H.; Aoyagi, T.; Morishima, H.; Matsuzaki, M.; Hamada, M. Pepstatin, a new pepsin inhibitor produced by *Actinomycetes*. *J. Antibiot.* (*Tokyo*) **1970**, *23* (5), 259–262.

(55) Nguyen, J. T.; Hamada, Y.; Kimura, T.; Kiso, Y. Design of potent aspartic protease inhibitors to treat various diseases. *Arch. Pharm.* (*Weinheim, Ger.*) **2008**, *341* (9), 523–535.

(56) Cunico, W.; Gomes, C. R. B.; Facchinetti, V.; Moreth, M.; Penido, C.; Henriques, M. G. M. O.; Varotti, F. P.; Krettli, L. G.; Krettli, A. U.; da Silva, F. S.; Caffarena, E. R.; de Magalhães, C. S. Synthesis, antimalarial evaluation and molecular modeling studies of hydroxyethylpiperazines, potential aspartyl protease inhibitors, part 2. *Eur. J. Med. Chem.* **2009**, *44* (9), 3816–3820.

(57) Orrling, K. M.; Marzahn, M. R.; Gutiérrez-de-Terán, H.; Åqvist, J.; Dunn, B. M.; Larhed, M. [alpha]-Substituted norstatines as the transition-state mimic in inhibitors of multiple digestive vacuole malaria aspartic proteases. *Bioorg. Med. Chem.* **2009**, *17* (16), 5933–5949.

(58) Lebon, F.; Ledecq, M. Approaches to the design of effective HIV-1 protease inhibitors. *Curr. Med. Chem.* **2000**, *7* (4), 455–477.

(59) Hidaka, K.; Kimura, T.; Ruben, A. J.; Uemura, T.; Kamiya, M.; Kiso, A.; Okamoto, T.; Tsuchiya, Y.; Hayashi, Y.; Freire, E.; Kiso, Y. Antimalarial activity enhancement in hydroxymethylcarbonyl (HMC) isostere-based dipeptidomimetics targeting malarial aspartic protease plasmepsin. *Bioorg. Med. Chem.* **2008**, *16* (23), 10049–10060.

(60) Noteberg, D.; Hamelink, E.; Hulten, J.; Wahlgren, M.; Vrang, L.; Samuelsson, B.; Hallberg, A. Design and synthesis of plasmepsin I and plasmepsin II inhibitors with activity in *Plasmodium falciparum*-infected cultured human erythrocytes. *J. Med. Chem.* **2003**, *46* (5), 734–746.

(61) Ersmark, B. S. A. H. Plasmepsins as potential targets for new antimalarial therapy. *Med. Res. Rev.* **2006**, *26* (5), 626–666.

(62) Alston, T. A.; Muramatsu, H.; Ueda, T.; Bright, H. J. Inactivation of gamma-cystathionase by gamma-fluorinated amino acids. *FEBS Lett.* **1981**, *128* (2), 293–297.

(63) Gelb, M. H.; Svaren, J. P.; Abeles, R. H. Fluoro ketone inhibitors of hydrolytic enzymes. *Biochemistry* **1985**, *24* (8), 1813–1817.

(64) Imperiali, B.; Abeles, R. H. Inhibition of serine proteases by peptidyl fluoromethyl ketones. *Biochemistry* **1986**, *25* (13), 3760–3767.

(65) Huang, L.; Lee, A.; Ellman, J. A. Identification of potent and selective mechanism-based inhibitors of the cysteine protease cruzain using solid-phase parallel synthesis. *J. Med. Chem.* **2002**, *45* (3), 676–684.

(66) Wood, W. J.; Huang, L.; Ellman, J. A. Synthesis of a diverse library of mechanism-based cysteine protease inhibitors. *J. Comb. Chem.* **2003**, *5* (6), 869–880.

(67) Caldera, P. S.; Yu, Z.; Knegtel, R. M.; McPhee, F.; Burlingame, A. L.; Craik, C. S.; Kuntz, I. D.; Ortiz de Montellano, P. R. Alkylation of a catalytic aspartate group of the SIV protease by an epoxide inhibitor. *Bioorg. Med. Chem.* **1997**, *5* (11), 2019–2027.

(68) Zutshi, R.; Chmielewski, J. Targeting the dimerization interface for irreversible inhibition of HIV-1 protease. *Bioorg. Med. Chem. Lett.* **2000**, *10* (17), 1901–1903.

(69) Lee, C. E.; Kick, E. K.; Ellman, J. A. General solid-phase synthesis approach to prepare mechanism-based aspartyl protease inhibitor libraries. Identification of potent cathepsin D inhibitors. *J. Am. Chem. Soc.* **1998**, *120*, 9735–9747.

(70) Bott, R.; Subramanian, E.; Davies, D. R. Three-dimensional structure of the complex of the *Rhizopus chinensis* carboxyl proteinase and pepstatin at 2.5-Å resolution. *Biochemistry* **1982**, *21* (26), 6956–6962.

(71) James, M. N.; Sielecki, A.; Salituro, F.; Rich, D. H.; Hofmann, T. Conformational flexibility in the active sites of aspartyl proteinases revealed by a pepstatin fragment binding to penicillopepsin. *Proc. Natl. Acad. Sci. U.S.A.* **1982**, *79* (20), 6137–6141.

(72) Johansson, P. O.; Chen, Y.; Belfrage, A. K.; Blackman, M. J.; Kvarnstrom, I.; Jansson, K.; Vrang, L.; Hamelink, E.; Hallberg, A.; Rosenquist, A.; Samuelsson, B. Design and synthesis of potent inhibitors of the malaria aspartyl proteases plasmepsin I and II. Use of solid-phase synthesis to explore novel statine motifs. *J. Med. Chem.* **2004**, *47* (13), 3353–3366.

(73) Johansson, P. O.; Lindberg, J.; Blackman, M. J.; Kvarnstrom, I.; Vrang, L.; Hamelink, E.; Hallberg, A.; Rosenquist, A.; Samuelsson, B. Design and synthesis of potent inhibitors of plasmepsin I and II: X-ray crystal structure of inhibitor in complex with plasmepsin II. *J. Med. Chem.* **2005**, *48* (13), 4400–4409.

(74) Silverman, R. B.; Abeles, R. H. Inactivation of pyridoxal phosphate dependent enzymes by mono- and polyhaloalanines. *Biochemistry* **1976**, *15* (21), 4718–4723.

(75) Crich, D.; Davies, J. W. Free-radical addition to di- and tripeptides containing dehydroalanine residues. *Tetrahedron* **1989**, *45*, 5641–5654.

(76) Takasaki, M.; Harada, K. Heterogenous assymetric hydrogenation of chiral dehydropeptides. *Chem. Lett.* **1984**, 1745–1746.

(77) Srinivasan, A.; Stephenson, R. W.; Olsen, R. K. Synthesis of dehydroalanine peptides from beta-chloroalanine peptide derivatives. *J. Org. Chem.* **1977**, *42* (13), 2253–2256.

(78) Fendrich, G.; Abeles, R. H. Mechanism of action of butyryl-CoA dehydrogenase: reactions with acetylenic, olefinic, and fluorinated substrate analogues. *Biochemistry* **1982**, *21* (26), 6685–6695.

(79) Guillerm, G.; Guillerm, D.; Vandenplas-Witkowki, C.; Rogniaux, H.; Carte, N.; Leize, E.; Van Dorsselaer, A.; De Clercq, E.; Lambert, C. Synthesis, mechanism of action, and antiviral activity of a new series of covalent mechanism-based inhibitors of *S*-adenosyl-L-homocysteine hydrolase. *J. Med. Chem.* **2001**, *44* (17), 2743–2752.
(80) Washtien, W.; Abeles, R. H. Mechanism of inactivation of gamma-cystathionase by the acetylenic substrate analogue propargylglycine. *Biochemistry* **1977**, *16* (11), 2485–2491.
(81) Abeles, R. H.; Maycock, A. L. Suicide enzyme inactivators. *Acc. Chem. Res.* **1976**, *9*, 313–319.
(82) Walsh, C. T. Suicide substrates, mechanism-based enzyme inactivators: recent developments. *Annu. Rev. Biochem.* **1984**, *53*, 493–535.
(83) Jacobi, P. A.; Brielmann, H. L.; Hauck, S. I. Synthesis of cyclic enamides by intramolecular cyclization of acetylenic amides. *Tetrahedron Lett.* **1995**, *36* (8), 1193–1196.
(84) Palfreyman, M. G.; Bey, P.; Sjoerdsma, A. *Enzyme Activated/Mechanism-Based Inhibitors*; The Biochemical Society: London, 1987; Vol. 23, pp 28−81.
(85) You, J.; Wroblewski, A. E.; Verkade, J. G. P[(*S*,*S*,*S*)-$CH_3NCH(CH_2Ph)CH_2]_3N$: a new C_3-symmetric enantiomerically pure proazaphosphatrane. *Tetrahedron* **2004**, *60*, 7877–7883.
(86) Kaltenbronn, J. S.; Stier, M. A. Separation of Diastereomers. U.S. Patent 4681972, 1987.
(87) Rich, D. H.; Sun, E. T.; Boparai, A. S. Synthesis of (3*S*,4*S*)-4-amino-3-hydroxy-6-methylheptanoic acid derivatives. Analysis of diastereomeric purity. *J. Org. Chem.* **1978**, *43* (18), 3624–3626.
(88) Rich, D. H.; Sun, E. T.; Ulm, E. Synthesis of analogues of the carboxyl protease inhibitor pepstatin. Effects of structure on inhibition of pepsin and renin. *J. Med. Chem.* **1980**, *23* (1), 27–33.
(89) Sheehan, J. C.; Hess, G. P. A new method of forming peptide bonds. *J. Am. Chem. Soc.* **1955**, *77* (4), 1067–1068.
(90) Anand, R. V.; Baktharaman, S.; Singh, V. K. A ring-closing metathesis approach toward formal total synthesis of (+)-diplodialide A. *J. Org. Chem.* **2003**, *68* (8), 3356–3359.
(91) Sheehan, J. C.; Ledis, S. L. Total synthesis of a monocyclic peptide lactone antibiotic, etamycin. *J. Am. Chem. Soc.* **1973**, *95* (3), 875–879.
(92) Sheehan, J. C.; Preston, J.; Cruickshank, P. A. A rapid synthesis of oligopeptide derivatives without isolation of intermediates. *J. Am. Chem. Soc.* **1965**, *87*, 2492–2493.
(93) Francis, S. E.; Banerjee, R.; Goldberg, D. E. Biosynthesis and maturation of the malaria aspartic hemoglobinases plasmepsins I and II. *J. Biol. Chem.* **1997**, *272* (23), 14961–14968.
(94) Hill, J.; Tyas, L.; Phylip, L. H.; Kay, J.; Dunn, B. M.; Berry, C. High level expression and characterisation of plasmepsin II, an aspartic proteinase from *Plasmodium falciparum*. *FEBS Lett.* **1994**, *352* (2), 155–158.
(95) Istvan, E. S.; Goldberg, D. E. Distal substrate interactions enhance plasmepsin activity. *J. Biol. Chem.* **2005**, *280* (8), 6890–6896.
(96) Luker, K. E.; Francis, S. E.; Gluzman, I. Y.; Goldberg, D. E. Kinetic analysis of plasmepsins I and II aspartic proteases of the *Plasmodium falciparum* digestive vacuole. *Mol. Biochem. Parasitol.* **1996**, *79* (1), 71–78.
(97) Grodberg, J.; Dunn, J. J. ompT encodes the *Escherichia coli* outer membrane protease that cleaves T7 RNA polymerase during purification. *J. Bacteriol.* **1988**, *170* (3), 1245–1253.
(98) Westling, J.; Cipullo, P.; Hung, S. H.; Saft, H.; Dame, J. B.; Dunn, B. M. Active site specificity of plasmepsin II. *Protein Sci.* **1999**, *8* (10), 2001–2009.
(99) Baker, B. R. *Design of Active-Site-Directed Irreversible Enzyme Inhibitors*; John Wiley & Sons: New York, 1967; pp 1−317.
(100) Siripurkpong, P.; Yuvaniyama, J.; Wilairat, P.; Goldberg, D. E. Active site contribution to specificity of the aspartic proteases plasmepsins I and II. *J. Biol. Chem.* **2002**, *277* (43), 41009–41013.
(101) Flotow, H.; Leong, C. Y.; Buss, A. D. Development of a plasmepsin II fluorescence polarization assay suitable for high throughput antimalarial drug discovery. *J. Biomol. Screening* **2002**, *7* (4), 367–371.
(102) Palamanda, J. R.; Casciano, C. N.; Norton, L. A.; Clement, R. P.; Favreau, L. V.; Lin, C.; Nomeir, A. A. Mechanism-based inactivation of CYP2D6 by 5-fluoro-2-[4-[(2-phenyl-1*H*-imidazol-5-yl)-methyl]-1-piperazinyl]pyrimidine. *Drug Metab. Dispos.* **2001**, *29* (6), 863–867.
(103) Wu, Y. Q.; Woster, P. M. Irreversible inhibition of human *S*-adenosylmethionine decarboxylase by the pure diastereomeric forms of *S*-(5′-deoxy-5′-adenosyl)-1-ammonio-4-methylsulfonio-2-cyclopentene (AdoMac). *Biochem. Pharmacol.* **1995**, *49* (8), 1125–1133.
(104) Kitz, R.; Wilson, I. B. Esters of methanesulfonic acid as irreversible inhibitors of acetylcholinesterase. *J. Biol. Chem.* **1962**, *237*, 3245–3249.
(105) Chen, K. X.; Njoroge, F. G.; Arasappan, A.; Venkatraman, S.; Vibulbhan, B.; Yang, W.; Parekh, T. N.; Pichardo, J.; Prongay, A.; Cheng, K. C.; Butkiewicz, N.; Yao, N.; Madison, V.; Girijavallabhan, V. Novel potent hepatitis C virus NS3 serine protease inhibitors derived from proline-based macrocycles. *J. Med. Chem.* **2006**, *49* (3), 995–1005.
(106) Deng, H. B.; Guang, W.; Wang, J. B. Selected cysteine residues in transmembrane domains of mu-opioid receptor are critical for effects of sulfhydryl reagents. *J. Pharmacol. Exp. Ther.* **2000**, *293* (1), 113–120.
(107) Desjardins, R. E.; Canfield, C. J.; Haynes, J. D.; Chulay, J. D. Quantitative assessment of antimalarial activity in vitro by a semiautomated microdilution technique. *Antimicrob. Agents Chemother.* **1979**, *16* (6), 710–718.
(108) Gluzman, I. Y.; Francis, S. E.; Oksman, A.; Smith, C. E.; Duffin, K. L.; Goldberg, D. E. Order and specificity of the *Plasmodium falciparum* hemoglobin degradation pathway. *J. Clin. Invest.* **1994**, *93* (4), 1602–1608.
(109) Liu, J.; Istvan, E. S.; Gluzman, I. Y.; Gross, J.; Goldberg, D. E. *Plasmodium falciparum* ensures its amino acid supply with multiple acquisition pathways and redundant proteolytic enzyme systems. *Proc. Natl. Acad. Sci. U.S.A.* **2006**, *103* (23), 8840–8845.
(110) Moura, P. A.; Dame, J. B.; Fidock, D. A. Role of *Plasmodium falciparum* digestive vacuole plasmepsins in the specificity and antimalarial mode of action of cysteine and aspartic protease inhibitors. *Antimicrob. Agents Chemother.* **2009**, *53* (12), 4968–4978.
(111) Zhao, H.; Sanda, F.; Masuda, T. Transformation of helical sense of poly(*N*-propargylamides) controlled by competition between structurally different enantiomeric amino acids. *Macromolecules* **2004**, *37* (24), 8888–8892.